

NAVAL POSTGRADUATE SCHOOL Monterey, California



**Transient Analysis of the 72 Inch TAC-4
Ruggedized Rack (CLIN 0003AA)
Subjected to Simulated Shock Loading**

by

Mark H. Oesterreich
Y. S. Shin

March 1998

19980512 008

Approved for public release; distribution is unlimited.

Prepared for: Naval Command, Control and Ocean Surveillance Center
Research Development Testing and Evaluation Division
71 Catalina Boulevard
San Diego, CA 92152-5000

Naval Postgraduate School
Monterey, California

RADM Robert C. Chaplin
Superintendent


R.S. Elster
Provost

This report was prepared in conjunction with research conducted for Naval Command ,
Control and Ocean Surveillance Center, Research Development Testing and Evaluation
Division.

This report was prepared by:

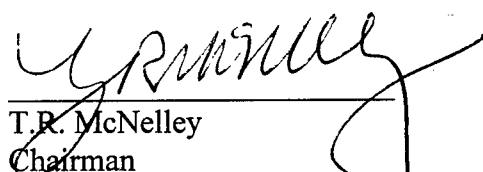


Mark H. Oesterreich
LT USN



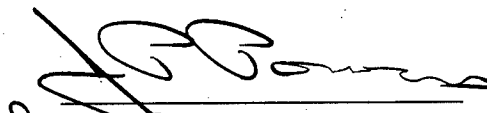
Y.S. Shin
Professor of Mechanical Engineering

Reviewed by:



T.R. McNelley
Chairman
Dept. of Mechanical Engineering

Released by:



D.W. Netzer
Dean of Research

DTIC QUALITY INSPECTED 3

REPORT DOCUMENTATION PAGE

Form Approved OMB No. 0704-0188

Public reporting burden for this collection of information is estimated to average 1 hour per response, including the time for reviewing instruction, searching existing data sources, gathering and maintaining the data needed, and completing and reviewing the collection of information. Send comments regarding this burden estimate or any other aspect of this collection of information, including suggestions for reducing this burden, to Washington Headquarters Services, Directorate for Information Operations and Reports, 1215 Jefferson Davis Highway, Suite 1204, Arlington, VA 22202-4302, and to the Office of Management and Budget, Paperwork Reduction Project (0704-0188) Washington DC 20503.

1. AGENCY USE ONLY <i>(Leave blank)</i>	2. REPORT DATE March 1998.	3. REPORT TYPE AND DATES COVERED FY 1998	
4. TITLE AND SUBTITLE: Transient Analysis of the 72 Inch TAC-4 Ruggedized Rack (CLIN 0003AA) Subjected To Simulated Shock Loading			5. FUNDING NUMBERS N6600196WR00036
6. AUTHOR(S) M.H. Oesterreich, Y.S. Shin			8. PERFORMING ORGANIZATION REPORT NUMBER NPS-ME-98-001
7. PERFORMING ORGANIZATION NAME(S) AND ADDRESS(ES) Naval Postgraduate School Monterey CA 93943-5000			
9. SPONSORING/MONITORING AGENCY NAME(S) AND ADDRESS(ES) NCCOSC, RDT&E Division, TAC Project Office			10. SPONSORING/MONITORING AGENCY REPORT NUMBER
11. SUPPLEMENTARY NOTES The views expressed here are those of the authors and do not reflect the official policy or position of the Department of Defense or the U.S. Government.			
12a. DISTRIBUTION/AVAILABILITY STATEMENT Approved for public release; distribution is unlimited.			12b. DISTRIBUTION CODE
13. ABSTRACT <i>(maximum 200 words)</i> The finite element modeling and subsequent static and modal analyses of the 72 Inch TAC-4 Rugged Rack computer system (CLIN 0003AA), as designed by Science Applications International Corporation (SAIC), was discussed in a previous report titled Modal Analysis of the 72 Inch TAC-4 Ruggedized Rack (CLIN 0003A). Follow-on transient analysis using these results have been performed to determine the rack's transient response to simulated shock inputs. This rack is designed to allow incorporation of commercial-off-the-shelf (COTS) computer systems for naval tactical computing requirements while still meeting MIL-STD-901D, the applicable military shock specification.			
14. SUBJECT TERMS TAC-4, transient analysis, shock simulation			15. NUMBER OF PAGES 45
			16. PRICE CODE
17. SECURITY CLASSIFICATION OF REPORT Unclassified	18. SECURITY CLASSIFICATION OF THIS PAGE Unclassified	19. SECURITY CLASSIFICATION OF ABSTRACT Unclassified	20. LIMITATION OF ABSTRACT SAR

NSN 7540-01-280-5500

Standard Form 298 (Rev. 2-89)
Prescribed by ANSI Std. Z39-18 298-102

Approved for public release; distribution is unlimited.

ABSTRACT

The finite element modeling and subsequent static and modal analyses of the 72 Inch TAC-4 Rugged Rack computer system (CLIN 0003AA), as designed by Science Applications International Corporation (SAIC), was discussed in a previous report titled Modal Analysis of the 72 Inch TAC-4 Ruggedized Rack (CLIN 0003AA). Follow-on transient analysis using these results have been performed to determine the rack's transient response to simulated shock inputs. This rack is designed to allow the incorporation of commercial-off-the-shelf (COTS) computer systems for naval tactical computing requirements while still meeting MIL-STD-901D, the applicable shock specification.

TABLE OF CONTENTS

1. INTRODUCTION.....	1
A. OVERVIEW.....	2
B. RESEARCH OBJECTIVES.....	2
2. TRANSIENT RESPONSE ANALYSIS METHOD.....	2
3. MODEL MODIFICATIONS.....	4
4. LARGE MASS METHOD OF ENFORCED.....	5
5. OTHER SIMULATION CONCERNS.....	10
6. TRANSIENT RESPONSE ANALYSIS.....	10
A. TUNED INPUT.....	12
B. SAMPLE INPUT.....	24
7. DISCUSSIONS.....	36
APPENDIX A, GENERAL MODEL CHARACTERISTICS.....	38
LIST OF REFERENCES.....	39
INITIAL DISTRIBUTION LIST.....	40

LIST OF FIGURES

Figure 1.	Finite Element Model of Rack Bullnose.	6
Figure 2.	Finite Element Model of Rack Mounts.	7
Figure 3.	Overview of Entire Rack Model.	8
Figure 4.	Locations of Nodes in Transient Response Graphs.	11
Figure 5.	Tuned Shock Base Input Acceleration vs. Time.	13
Figure 6.	Acceleration Response of Node 6707 (Front/Bottom Mount).	14
Figure 7.	Acceleration Response of Node 6887 (Rear/Bottom Mount)..	15
Figure 8.	Acceleration Response of Node 4332 (Power Supply)	16
Figure 9.	Acceleration Response of Node 241 (Power Distribution Unit).	17
Figure 10.	Acceleration Response of Node 2531 (Monitor)	18
Figure 11.	Acceleration Response of Node 6542 (CPU)	19
Figure 12.	Acceleration Response of Node 4220 (Bullnose)	20
Figure 13.	Acceleration Response of Node 520.	21
Figure 14.	Displacement of Node 6846 (Front/Bottom Mount).	22
Figure 15.	Displacement of Node 6850 (Rear/Bottom Mount).	23
Figure 16.	Sample Shock Base Excitation vs. Time	25
Figure 17.	Acceleration Response of Node 4332 (Power Supply).	26
Figure 18.	Acceleration Response of Node 241 (Power Distribution Unit).	27
Figure 19.	Acceleration Response of Node 2531 (Monitor).	28
Figure 20.	Acceleration Response of Node 6542 (CPU)	29
Figure 21.	Acceleration Response of Node 4220 (Bullnose)	30
Figure 22.	Acceleration Response of Node 537 (Bottom of Cabinet).	32
Figure 23.	Acceleration Response of Node 6193 (Top of Cabinet).	33
Figure 24.	Displacement Response of Node 6846 (Front/Bottom Mount).	34
Figure 25.	Displacement Response of Node 6850 (Rear/Bottom Mount).	35

1. INTRODUCTION

A. OVERVIEW

The rapid pace of current electronic and computer modernization coupled with the slow turnaround and life-cycle outlook of traditional naval contracting has precipitated a situation where the navy can not keep pace with current technology. As a further difficulty in the contracting process, all military-specifications (mil-specs) must be met by the manufacturer. This adds significant cost and design and manufacturing delays to any computer system required for naval tactical use. These design, manufacture, and contracting delays result in a product which is obsolete well before it can be placed into service.

To remedy this situation, the U.S. Navy has changed its contracting procedures, but more importantly the type of computer hardware used for tactical computing. Previously, each tactical computer was a stand-alone unit specifically designed for its requisite task, or relied on a standard chassis which was modified to perform the required task (e.g. AN-UYK-7,-43). This approach was satisfactory until the advent of the computer revolution which heralds a new technical innovation or increase in computing capacity about every six months. This time period is too short for the industry to design shock proof computers at the same rate as commercial computers improve. The Navy is now implementing the use of COTS computers in tactical applications.

The benefits of this introduction of this commercially based strategy will reduce delays in introducing new technology to the fleet, reduce software development and logistics costs, and improve long-term compatibility and reusability of tactical information technology investments. However, the survivability of COTS in various types of severe environments is questionable. The TAC family uses commercial computers and places them into special ruggedized racks which are designed to meet all of the applicable mil-specs thereby allowing the use of COTS equipment in a tactical environment.

B. RESEARCH OBJECTIVES

There are three different sizes of ruggedized racks used in the TAC-4 system, each size rack also has varying equipment types and configurations. In this work, the analysis is focused on the 72 inch TAC-4 rack with the CLIN 003AA configuration which has already begun testing for its compliance with the shock and vibration mil-specs (MIL-S-901D and MIL-S-167-1). Due to the nature of the use of this computer system, the rack must reduce all specified shocks and vibrations to a level that the non-hardened commercial computer hardware can handle without system failure (interruption of service).

The purpose of this study is to perform two finite element transient analyses of CLIN 0003AA (as developed by SAIC [Reference 1]) using a refinement of the model developed previously in Reference 2. The two analyses include a tuned 'generic barge shock' input and an actual shock input used in a biomechanic response study (the actual barge testing of the rack has not been completed yet).

2. MODAL TRANSIENT RESPONSE ANALYSIS METHOD

The following discussion is for the generalized case of transient response analysis. This study is strictly a base excitation problem which requires a slight modification to this discussion, specifically in the description of the excitation force vector $\{F\}$. This modification will be discussed further in Section 4, entitled The Large Mass Method.

The previous modal analysis of the rack resulted in n eigenpairs of ω_n (eigenvalue) and $\{\phi^n\}$ (eigenvector or mode shape) which will be subsequently used to decouple the system differential equations. This decoupling drastically simplifies the response calculations for the system. Because each eigenvector is orthogonal to every other eigenvector it allows vibration response to be described as a linear combination of these mode shapes. By constructing a square transformation matrix whose columns consist of the n mode shapes, $[\phi^1 \phi^2 \dots \phi^n]$ or $[\Phi]$. The use of the transformation matrix

allows the physical system coordinates to be transformed into the modal system coordinates by substituting for $\{q(t)\}$, the physical coordinate vector, in

$$[M]\{\ddot{q}\} + [C]\{\dot{q}\} + [K]\{q\} = \{F\} \quad (1)$$

with

$$\{q(t)\} = [\Phi]\{u(t)\} \quad (2)$$

where $\{u(t)\}$ is the modal coordinate vector. Premultiplying the entire equation through with $[\Phi]^T$ produces:

$$[M]\{\ddot{u}\} + [C]\{\dot{u}\} + [K]\{u\} = \{F\} \quad (3)$$

where $[M]$ is the diagonalized mass matrix, $[C]$ is the diagonalized damping matrix, $[K]$ is the diagonalized stiffness matrix and $\{F\}$ is the modal Force vector. This process of diagonalizing these matrices is known as modal decomposition and results in n independent equations, one for each modal degree of freedom (DOF). The i^{th} DOF's equation corresponds to the i th row of Equation (3) and may be written as:

$$M_{ii}\ddot{u}_i + C_{ii}\dot{u}_i + K_{ii}u_i = F_i \quad (4)$$

Premultiplying Equation (3) through by $\frac{1}{[M]}$ results in:

$$\{\ddot{u}\} + [2\zeta_i\omega_i]\{\dot{u}\} + [\omega_i^2]\{u\} = \{a\} \quad (5)$$

where ζ_i is the i^{th} modal damping factor, ω_i is the i^{th} natural frequency and $\{a\}$ is the time varying base acceleration vector produced by the forcing function.

The i^{th} row of the uncoupled system of equations (with time dependence added for emphasis) is now:

$$\ddot{u}_i(t) + 2\zeta_i\dot{u}_i(t) + \omega_i^2 u_i(t) = a_i(t) \quad (6)$$

The solution to Equation (1) requires two initial conditions of the form:

$$\{q\}_{t=0} = \{q_0\} \quad (7)$$

and

$$\{\dot{q}\}_{t=0} = \{\dot{q}_0\} \quad (8)$$

These equations must also be transformed into modal coordinates. This is accomplished in a similar manner as the equations of motion for the system resulting in:

$$\{u_0\} = [M]^{-1}[\Phi]^T[M]\{q_0\} \quad (9)$$

and

$$\{\dot{u}_0\} = [M]^{-1}[\Phi]^T[M]\{\dot{q}_0\} \quad (10)$$

By applying these transformed initial conditions to Equation (6), a solution for the modal displacements is obtained of the form:

$$u_i(t) = u_{0i} \cos(\omega_i t) + \frac{1}{\omega_i} \dot{u}_{0i} \sin(\omega_i t) + \frac{1}{\omega_i} \int_0^t a_i(\tau) \sin \omega_i(t - \tau) d\tau \quad (11)$$

Each modal coordinate has a solution of this form and then these are combined into vector form. The physical displacements are then obtained using Equation (2):

$$\{q(t)\} = [\Phi]\{u(t)\}$$

This method as shown here works well for models with up to a few hundred DOF, however becomes extremely cumbersome for larger models. Only a slight modification is required to remedy this situation. Most of the system transient response is contained in the lower frequency mode shapes, therefore a very accurate approximation of the system response can be made using a relatively small proportion of the total mode shapes. This is known as modal truncation and is done by modifying Equation (2) as follows:

$$\{q(t)\} = [\Phi]\{q(t)\} \cong \sum_{i=1}^{NDOF} \{\phi_i\} q_i(t) \quad (12)$$

Here, NDOF is the total number of mode shapes used in the approximation.

3. MODEL MODIFICATIONS

The model used for the transient analysis was modified from the model used in the modal analysis in three important respects. First, the bullnose containing the system keyboard and track ball was added. Second, the system's shock mounts were also added. Finally, the cabinet's rear panel was subdivided to better represent the true system configuration.

The bullnose and its mounting brackets were added to the front of the rack. The brackets were modeled using shell elements which act as a simple interface between the bullnose and the rack frame. In the case of the bullnose, the structure was simplified into solid block elements of the appropriate size and density to ensure the correct weight. As before bolt holes, electrical connectors, knobs, etc. were not transferred to the model because the gross response is what of interest. This also minimized the number of nodes in the model which speeds up all calculations. Figure 1 shows the finite element model of the bullnose.

The system shock mounts were also idealized. This consisted of connecting the appropriate nodes on the cabinet using rigid beam elements, maintaining the correct geometric offsets, to the coincident nodes used for the spring elements. Each mount model uses three springs one in each translational direction. The manufacturer supplied mount force-displacement curves[Reference 3] were then used to obtain the spring constant values for each of these springs. Because no rotational data was available, rotational spring stiffness was not modeled. For this model, a linear approximation for each spring stiffness was used. Figure 2 shows how the mounts were modeled.

The subdivision of the back panel was the result of the initial modal analysis showing that the rear panel was not responding appropriately and therefore affecting the response of the rest of the system.

Once these modifications were complete, the model was again checked to ensure that no duplicate nodes or elements existed, the dimensions and material properties were correct, and that the appropriate free edges were present. Figure 3 shows an overview of the entire finite element model and Appendix A lists the general model characteristics.

4. LARGE MASS METHOD OF ENFORCED MOTION

The generalized base excitation problem requires that the excitation force vector $\{F\}$ be defined as the base mass times the acceleration (the appropriate derivatives are taken if the actual input is defined as a displacement or velocity time history). In this

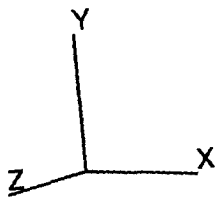
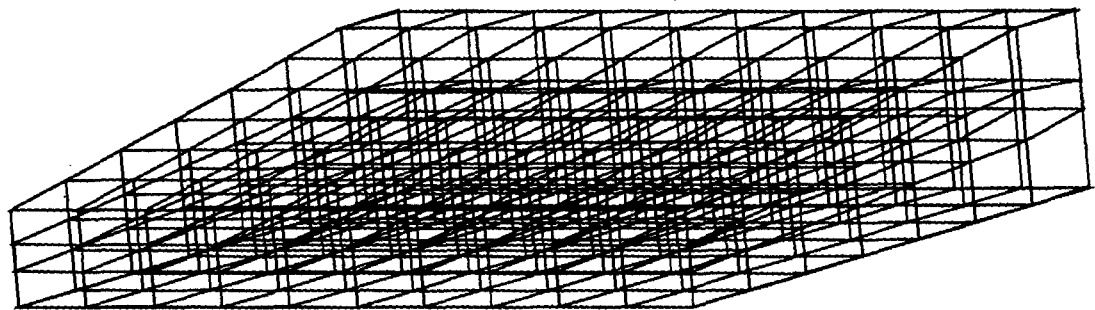


Figure 1. Finite Element Model of Rack Bullnose

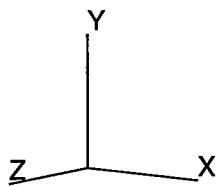
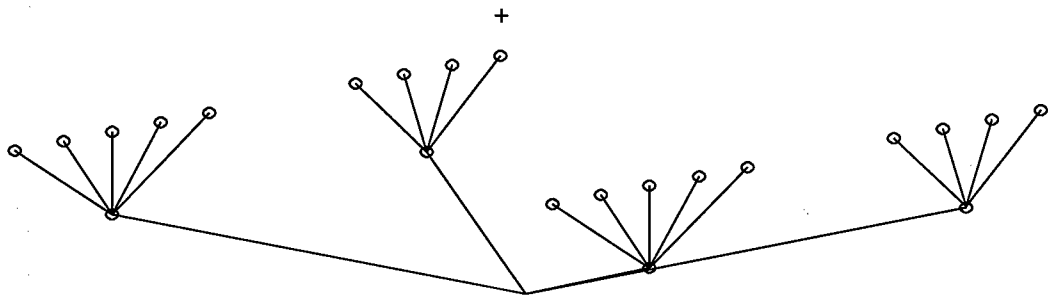


Figure 2. Finite Element Model of Rack Mounts

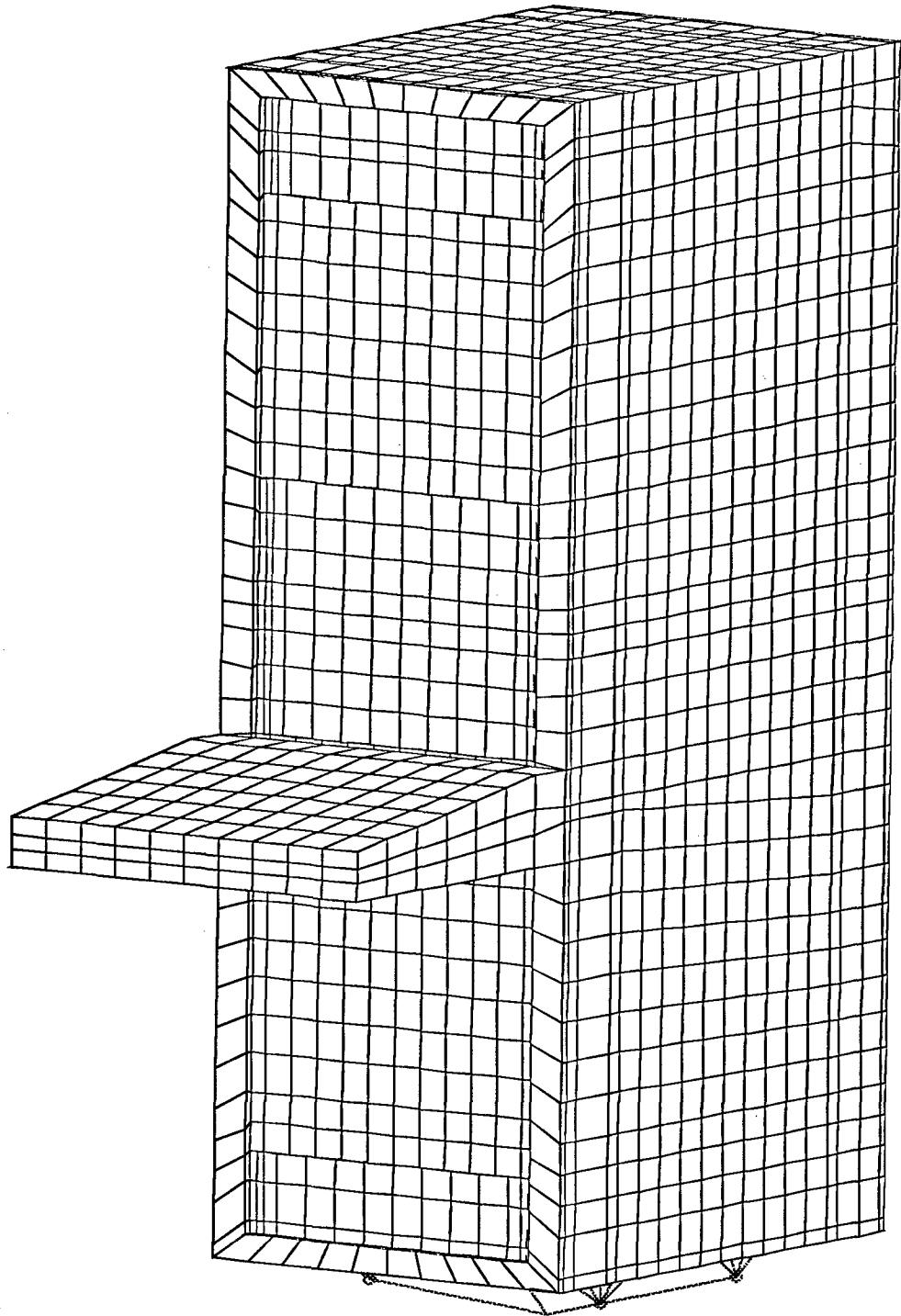


Figure 3. Overview of Entire Rack Model

analysis, the actual physical base mass is unknown, so it is assumed as a very large value. This ensures that any errors in calculations remain insignificant.

All transient response analyses of the model were performed using the Modal Transient Response Method incorporating the Large Mass Method for use within the MSC/NASTRAN finite element structural analysis code. The Large Mass Method (LMM) is required when the actual applied forces to the structure are physically unmeasurable, but rather measured as an enforced motion (displacement, velocity, or acceleration). This situation is known as base excitation. The LMM is a method of converting these motions into equivalent forces for use in the matrix equation of motion, Equation 1, for use within NASTRAN's transient analysis routine.

The LMM is implemented by placing large point masses (m_0) for all enforced degrees of freedom. These masses should be several orders of magnitude larger than the structural mass (typically 10^6 times larger) which ensures sufficient numerical accuracy. For the current analyses, the enforced motions are specified as a base acceleration time history, $\ddot{x}(t)$. The converted force is now simply $P = m_0\ddot{x}(t)$ at each enforced DOF.

One problem that arises in the LMM is the fact that you have added mass to the system which is not physically there. Therefore, care must be taken in the NASTRAN input deck to ensure that the force is then scaled back down by the same factor as the magnitude of the point masses to ensure that the addition of these point masses does not affect the results. Another problem that can arise with the large mass method is the possibility of removing the static determinacy of the model, thereby introducing rigid body modes (RBMs) into the solution. Rigid body modes are undeformed gross translation or rotation of the entire model which are not present in the rack's physical system since it is attached to the "ground". This problem is avoided by purposely not including these RBMs in the calculation of the system response. Since RBMs manifest themselves in the modal analysis by having a characteristic zero natural frequency ($\omega_n=0$), they can easily be excluded from the solution by specifying a modal frequency range starting from a value slightly larger than zero in the NASTRAN input deck. With these two problems averted, NASTRAN can now effectively solve for the transient solutions.

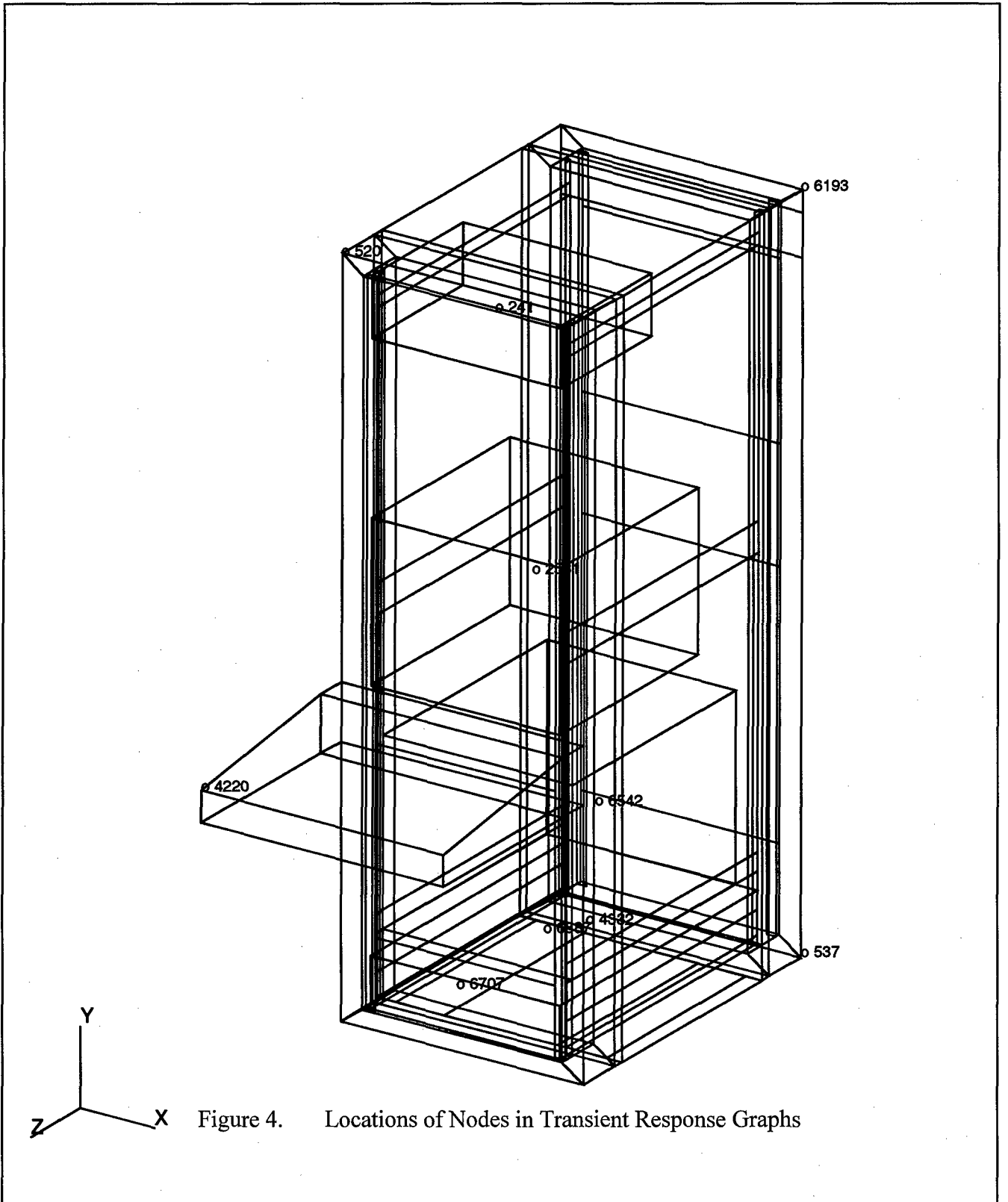
5. OTHER SIMULATION CONCERNS

There are also two more things that are important when using Modal Transient Response Analysis, the integration time step and cut-off frequency. The cut-off frequency is the frequency above which the mode shapes have a minimal effect on the system response. 200Hz was chosen to ensure that enough mode shapes were used in the solution to ensure calculational accuracy and also would capture the characteristics of the input acceleration time history. As for the time step, the most important concern is to capture both the characteristics of the input and that it is small enough show the characteristics of the highest modal response frequency used. For the halfsine input a time step of .001 seconds was used, while for the sample deck input a time step of .002 seconds was used. Although this a shorter time step for this analysis was preferred, a limitation on computer storage resources required a shorter time step.

6. TRANSIENT RESPONSE ANALYSIS

Two separate analysis of the model were performed. The first analysis used an idealized shock input which represents a generic shock designed to get the feel of the system response. This consisted of a 40g, 2msec, half sine wave shock pulse. The second analysis used an actual shock input acceleration obtained from a barge test performed for human response trials. Although it is probable that this input will have no correlation with the actual barge test input, it is useful to show how the rack responds to an actual shock input.

The following results show to varying degrees how well the rack system mitigates the shock acceleration of the various portions of the rack. Throughout the discussion it is important to note that in the case of both shock inputs, the results were purposely guided towards theoretical conservatism (worst possible case). These results can only be verified through actual physical testing which is scheduled for the future. Refer to Figure 4 for the approximate location of all nodes mentioned in the discussion.



A. TUNED INPUT

Figure 5 is a plot of the 2msed shock impulse used for this analysis. All responses were calculated out to 1 second to ensure that the peak responses were captured. Figures 6 and 7 show the acceleration response of portions of the top of the base shock mounts with Figure 6 being the front-bottom mount (NODE 6707) and Figure 7 the rear-bottom mount (NODE 6887). For both of these figures, the initial shock input pulse is mitigated somewhat (by 12 and 8 Gs respectively), and is then rapidly damped down (with a ring-down effect to evident to varying degrees) to approximate 3G peaks at each node location. This shows that the shock mounts are effective for this type of input pulse.

The rack system is designed to mitigate shock to the electronic components. Figures 8 through 11 are the acceleration time responses for representative nodes in each of the electronic components mounted within the rack, corresponding to the Power Supply, Power Distribution Unit, Monitor, and Central Processing Unit respectively. For all of these components the peak shock value is mitigated by about 12 Gs. Although the peak value is still around 28 G's for each component, this equates to a 30% reduction from the input peak. Also as in the case of the mounts, the shock value is rapidly mitigated to 3 G peaks. Figure 12 shows the acceleration response of NODE 4220 at the tip of the bullnose. Here, the initial input impulse is mitigated to about 31 Gs. This is higher than the other electronic components due to the location of this node being extended out far from the system's center of gravity, acting as a cantilever. This node was chosen to represent the largest response in the bullnose. As in the other electronic components, the shock is quickly mitigated down, however these peaks are higher at about 4.5 Gs due to the cantilever effect.

Figure 13 shows the acceleration response of the upper-left front corner of the rack. This node was chosen to represent how the cabinet structure itself responds to the shock loading. The peak response for NODE 520 is mitigated by approximately 11.5 Gs and quickly is mitigated down to 3 G peaks as discussed before.

The next major area of concern with the rack is to determine if the shock mounts themselves will exceed design limits or bottom out. Figure 14 shows the magnitude of the displacement response of the front-bottom mount (NODE 6846), while Figure 15

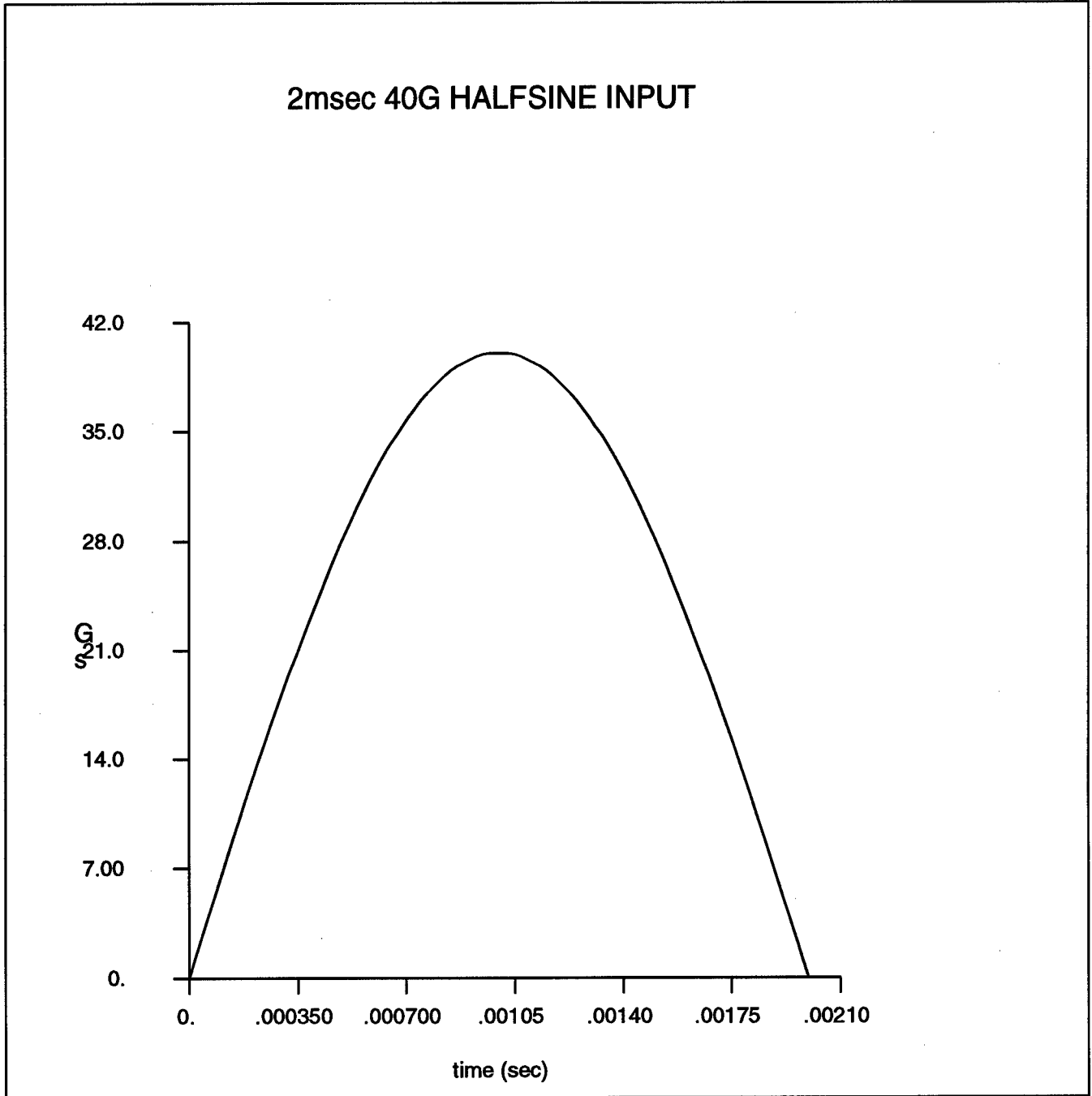


Figure 5. Halfsine Shock Base Input Acceleration vs. Time

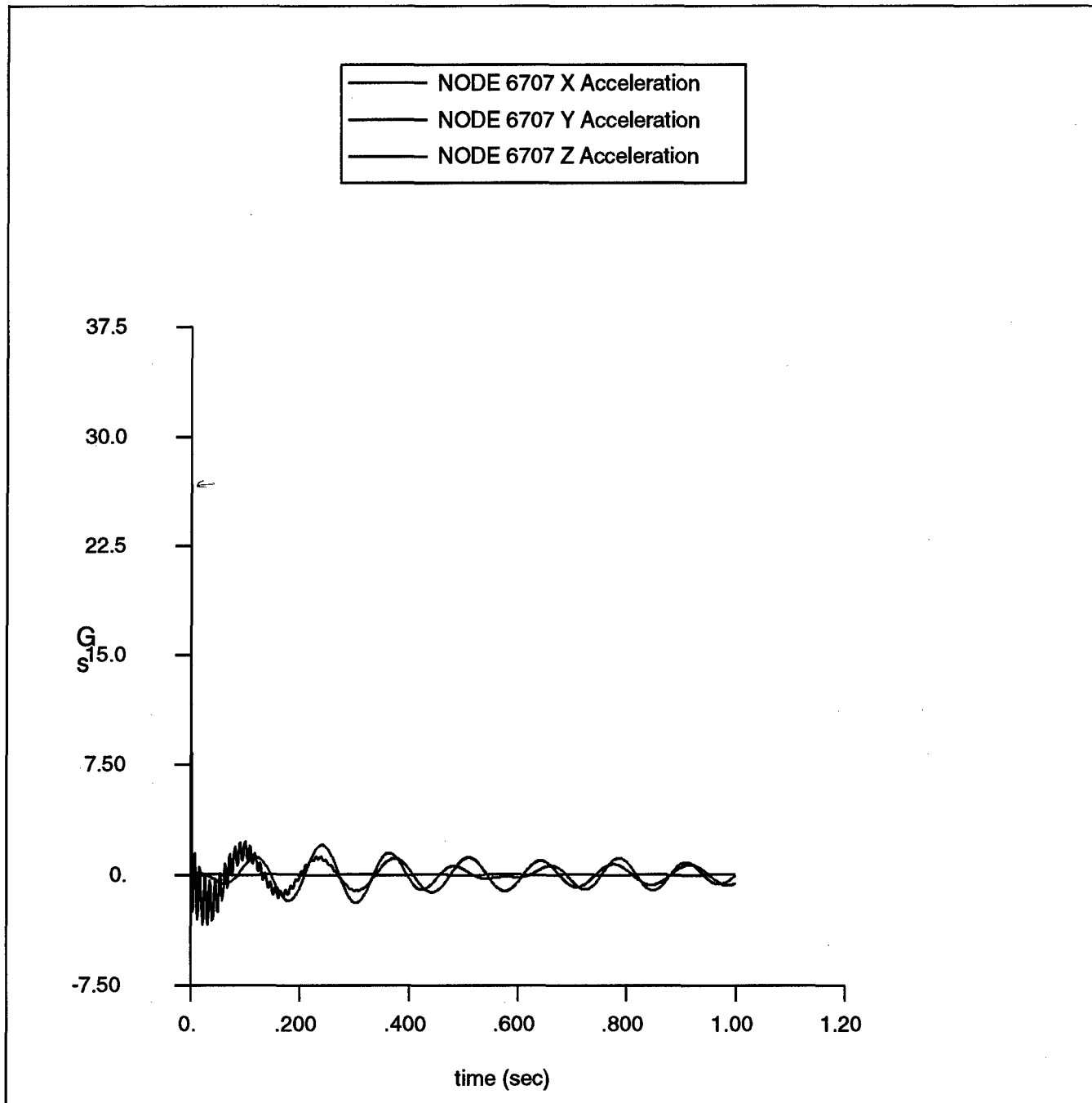


Figure 6. Acceleration Response of Node 6707 (Front/Bottom Mount).

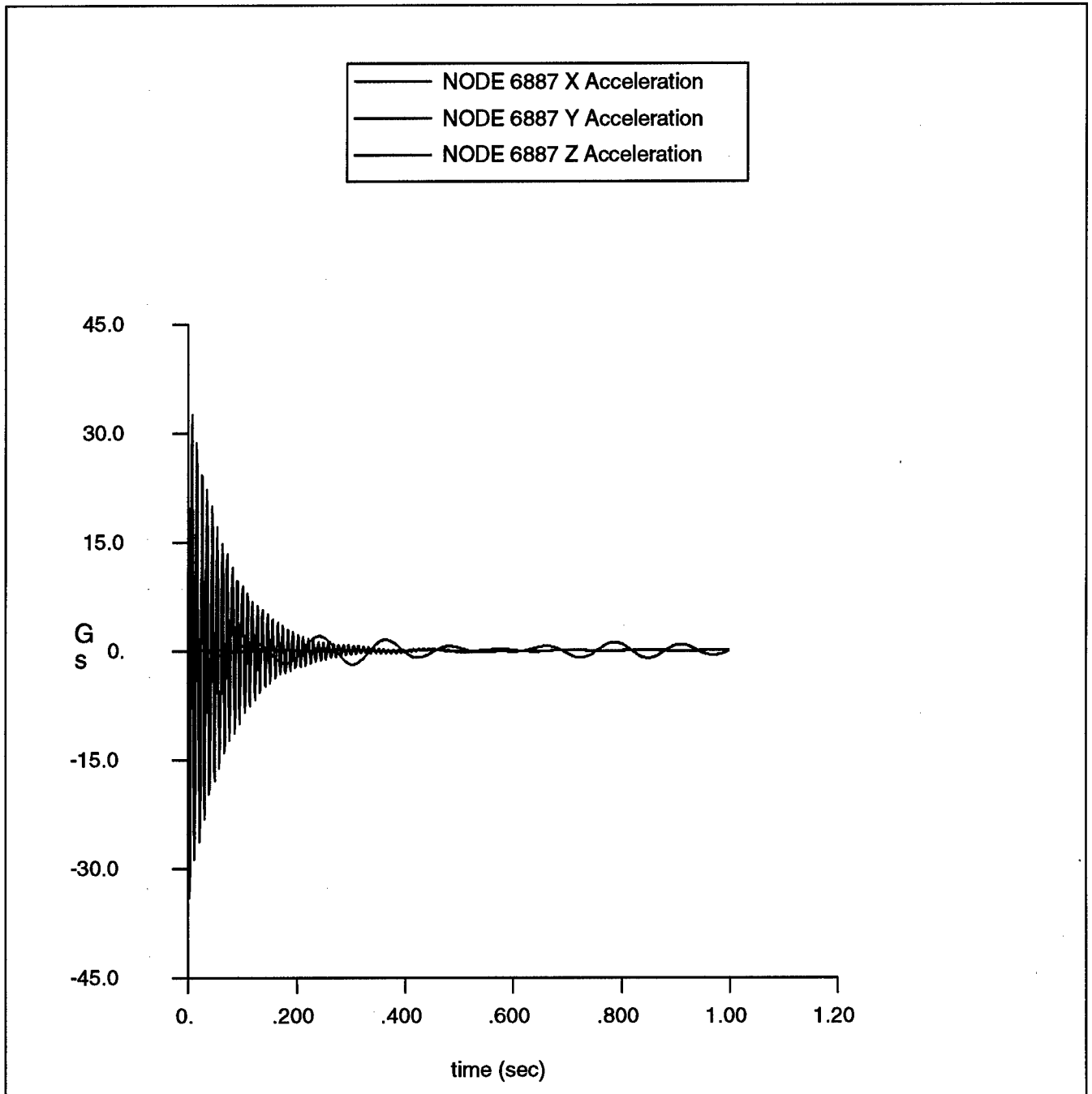


Figure 7. Acceleration Response of Node 6887 (Rear/Bottom Mount)

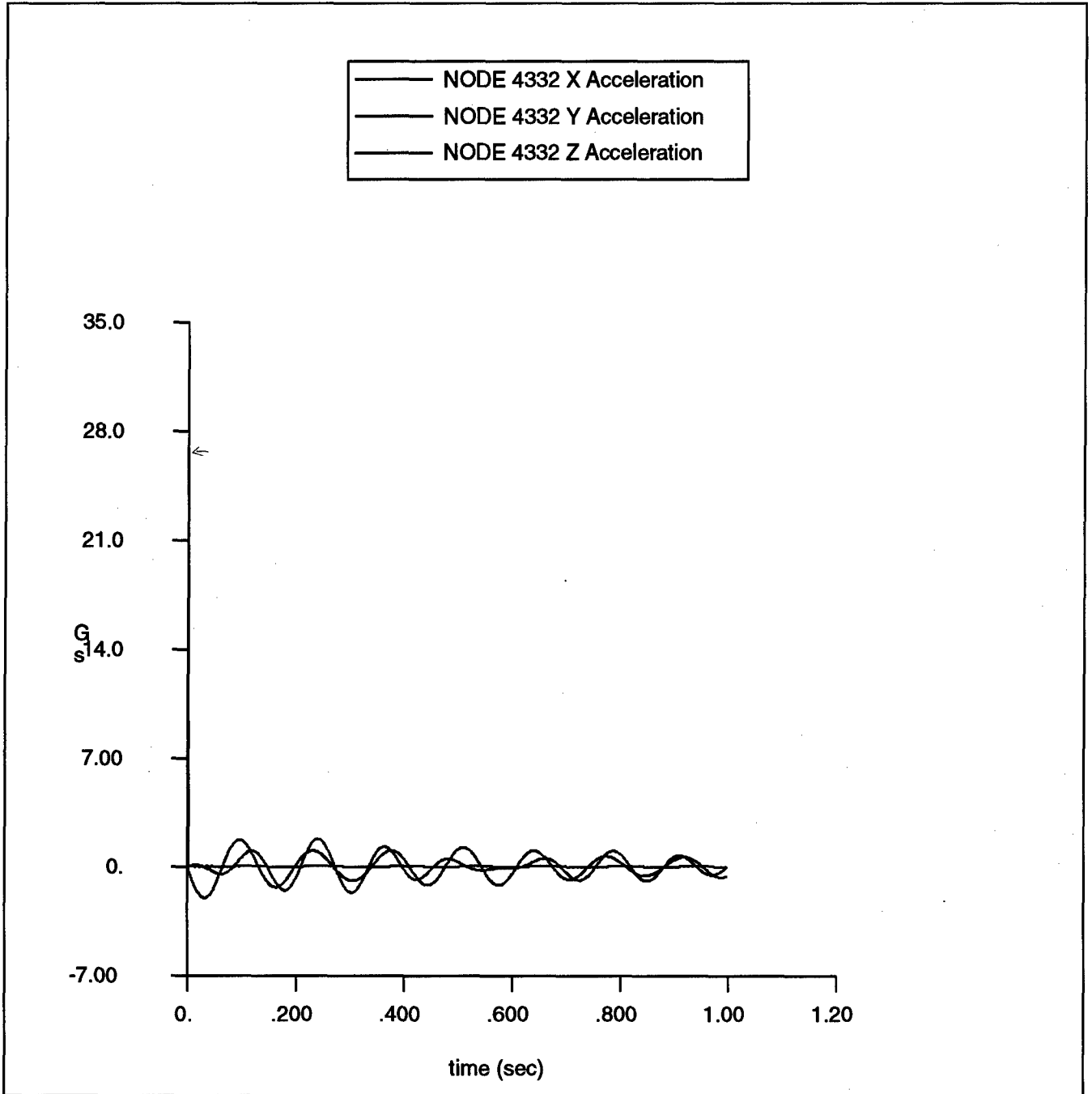


Figure 8. Acceleration Response of Node 4332 (Power Supply)

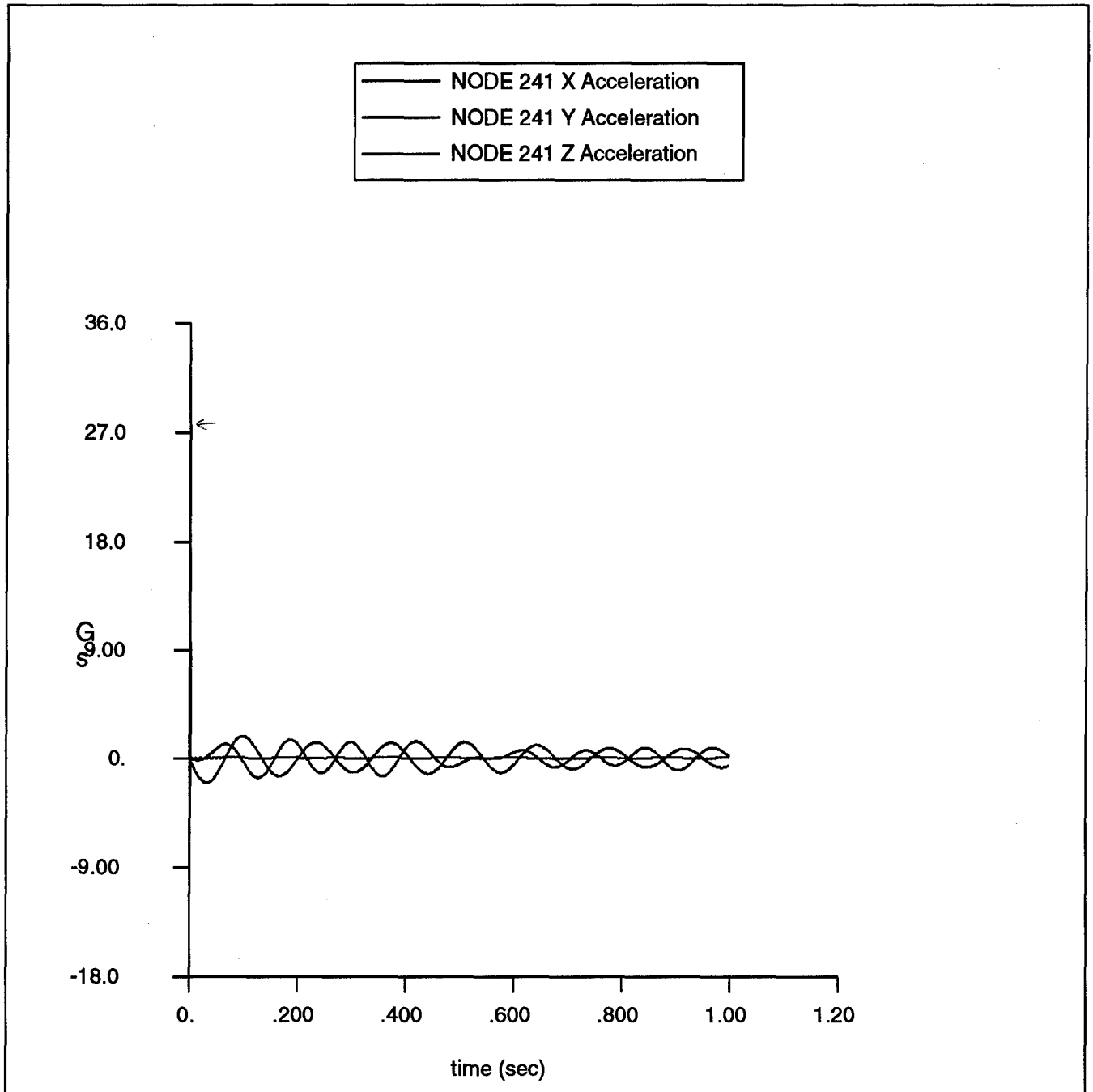


Figure 9. Acceleration Response of Node 241 (Power Distribution Unit)

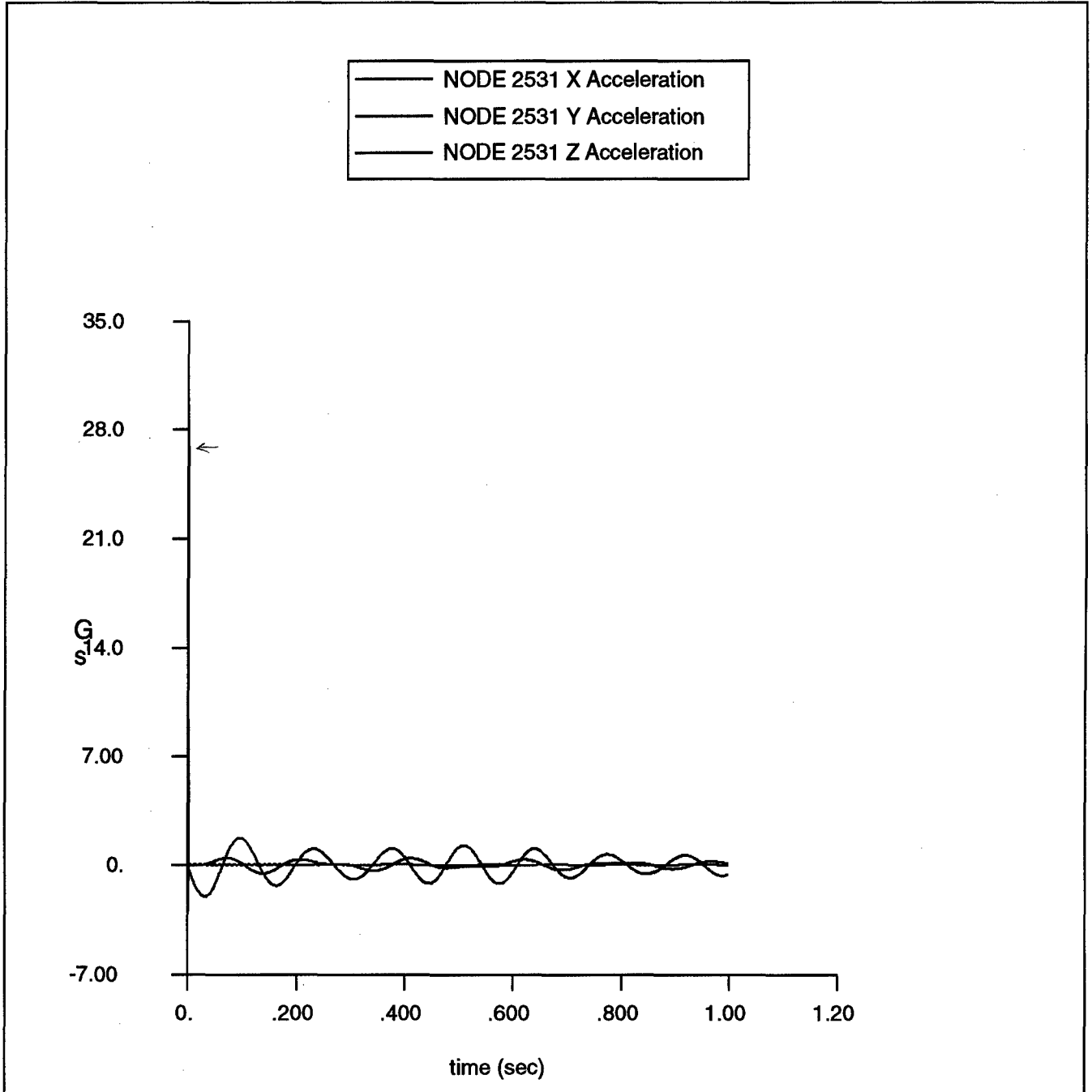


Figure 10. Acceleration Response of Node 2531 (Monitor)

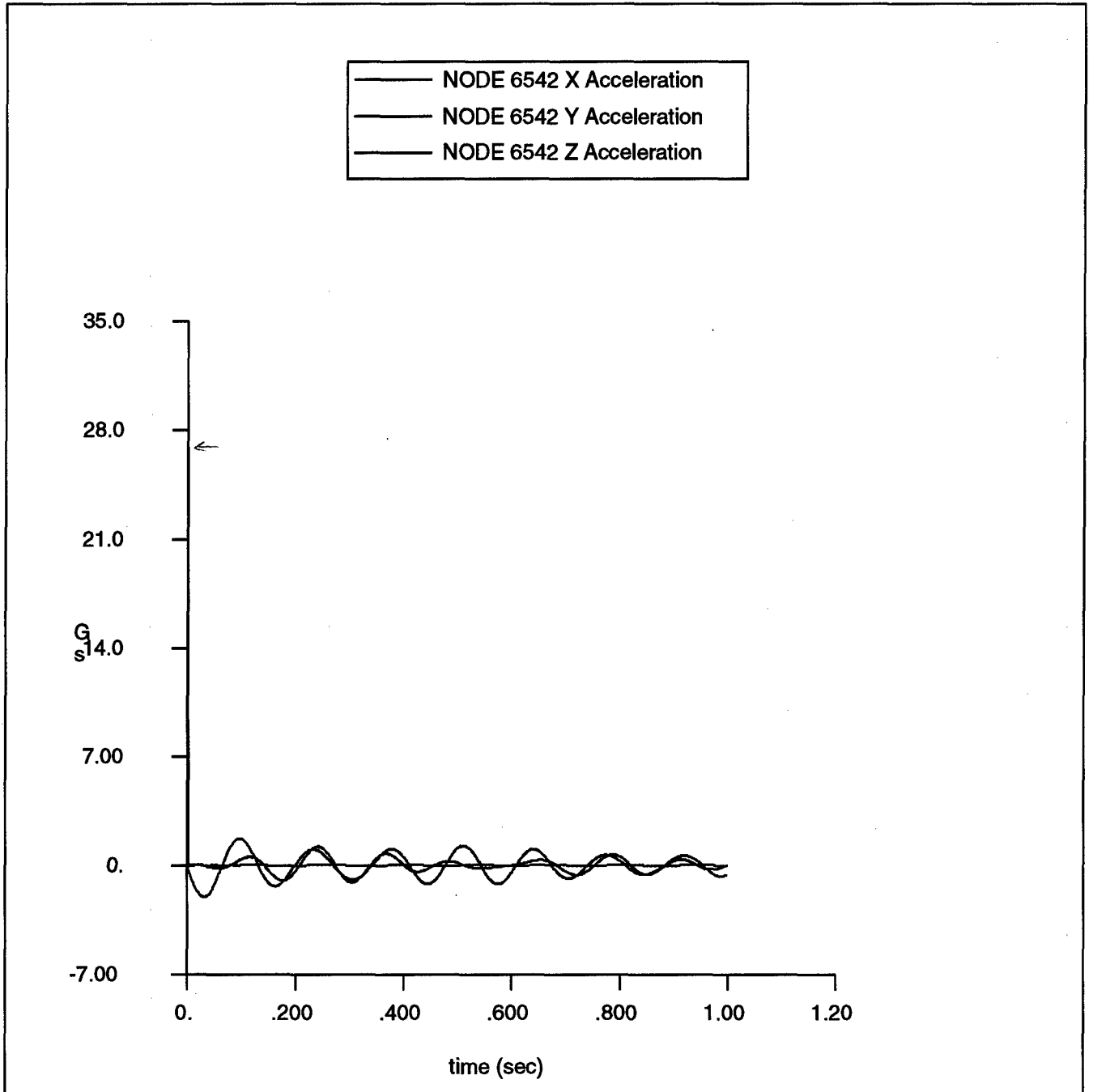


Figure 11. Acceleration Response of Node 6542 (CPU)

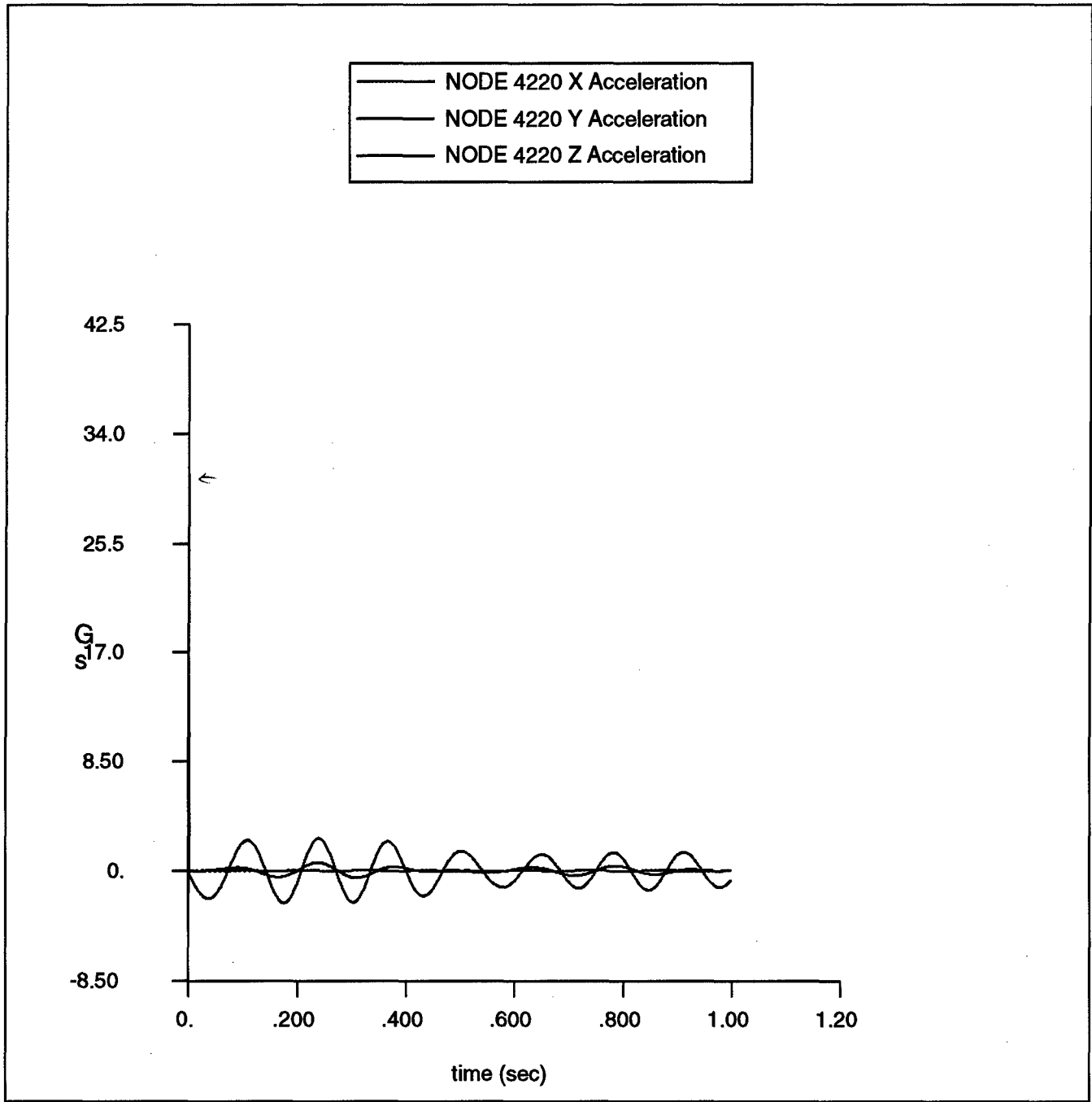


Figure 12. Acceleration Response of Node 4220 (Bullnose)

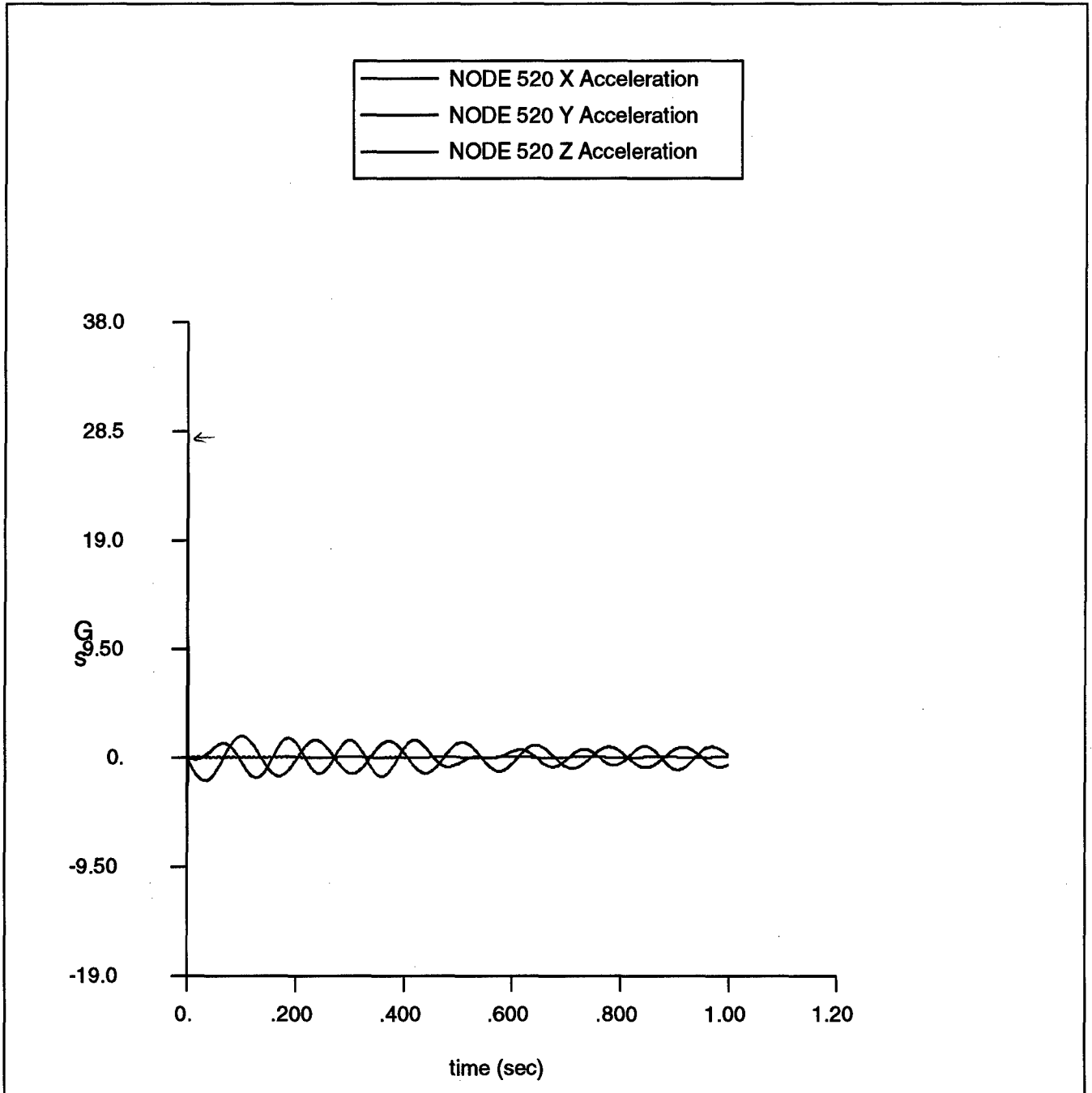


Figure 13. Acceleration Response of Node 520 (Top/Front Left Corner)

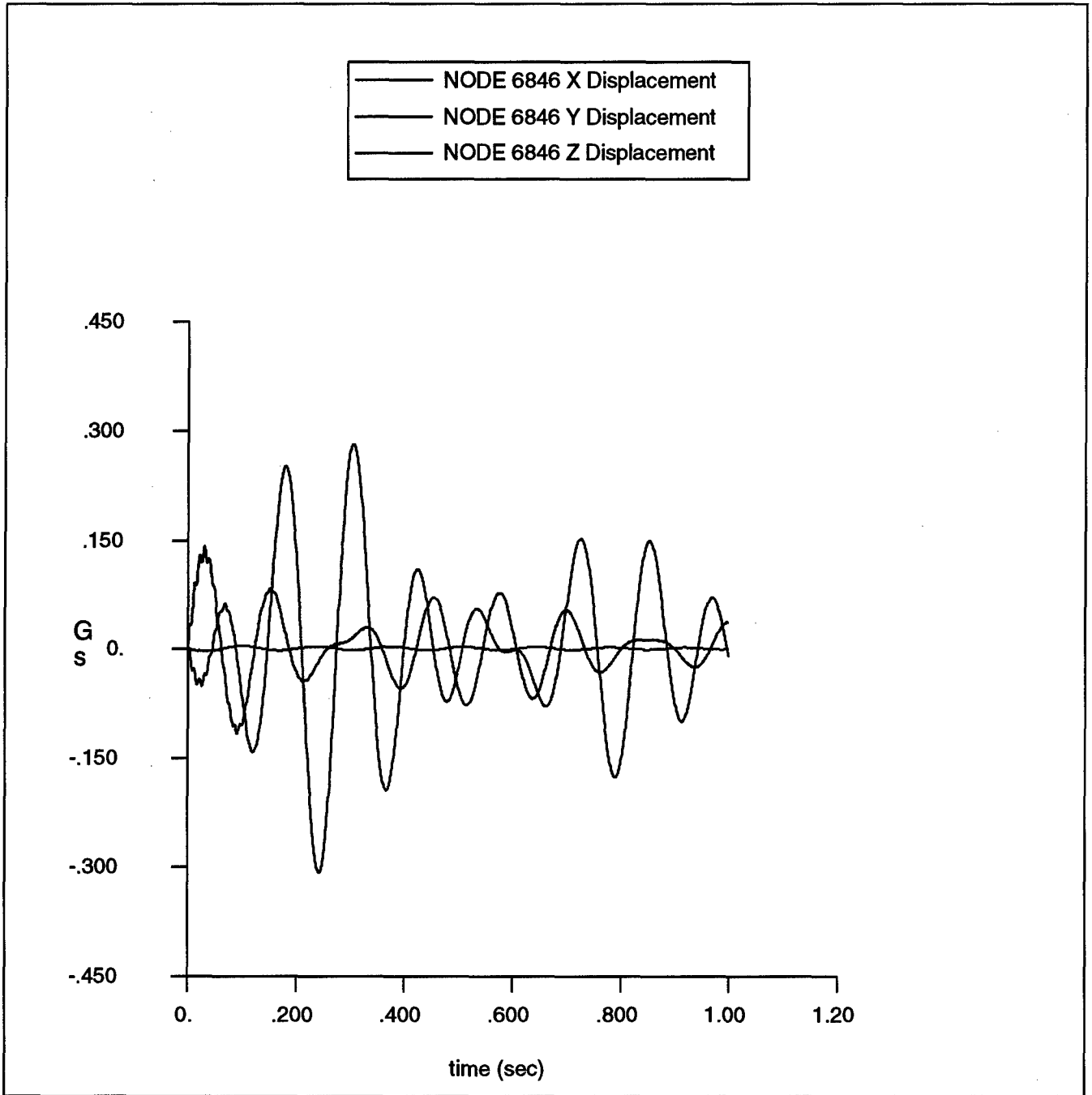


Figure 14. Displacement of Node 6846 (Front/Bottom Mount)

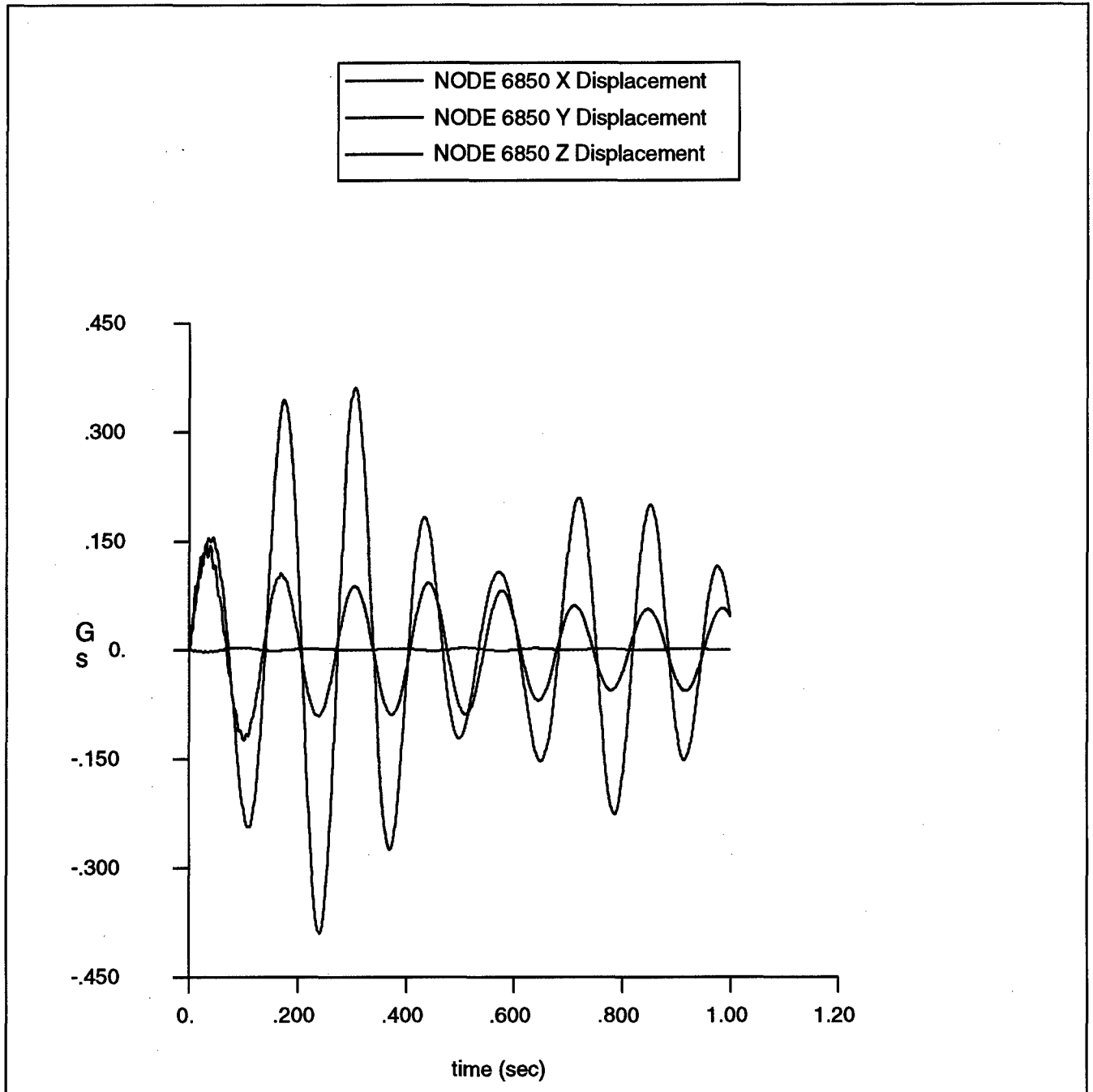


Figure 15. Displacement of Node 6850 (Rear/Bottom Mount).

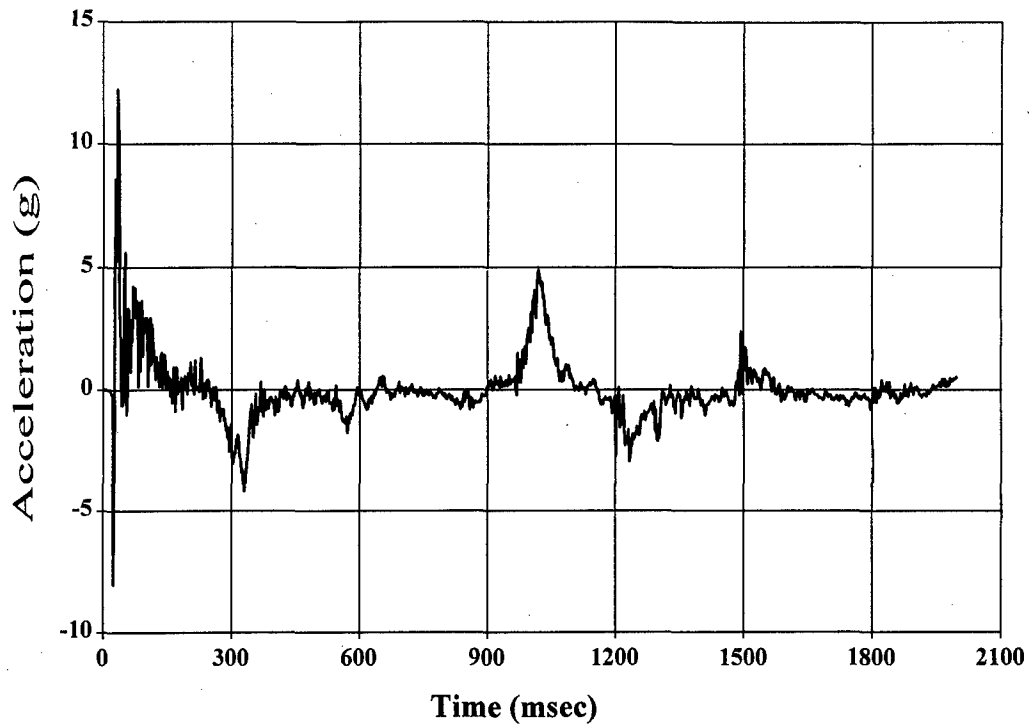
shows the same for the rear-bottom mount (NODE 6850). The Y Displacement curve corresponds to the vertical direction, Z Displacement to front/back motion and X displacement to side/side motion. Of concern, however, is the Z Displacement (front/rear direction) whose considerable motion with respect to the other two directions indicates a transference of energy from the Y to the Z direction. This warrants a closer analysis using the actual non-linear spring characteristics instead of the current linear approximation. This must be done prior to any definite conclusions being drawn from this data.

B. SAMPLE INPUT

Figure 16 shows the shock input time history in both the vertical and horizontal (fore/aft) directions from the human shock response test data [Reference 4]. For this analysis case, responses were calculated out to two seconds because this was the available length of time history for the shock input. This input is significantly different from the previous one because shock energy is added to the rack system over the entire two second time period, rather than for a brief period at the beginning of the time period as in the halfsine input.

Again, the electronic components are of extreme interest. Figures 17 through 20 show the response time histories for representative nodes for the electronic components mounted with the cabinet, corresponding to the Power Supply, Power Distribution Unit, Monitor, and Central Processing Unit respectively. Figure 21 shows the acceleration response of the end of the bullnose. The response amplitudes for all of these electronic components generally increase over the entire time history. This is due to the addition of shock energy throughout the entire time period. This acts to provide constructive and destructive response compounding of the system, reinforcing some peaks and mitigating others within the time response history. As with the halfsine input case, the initial peak input values for the electronic components are mitigated by approximately 30%, with the exception of the bullnose whose initial peak value is higher due to its cantilevered position.

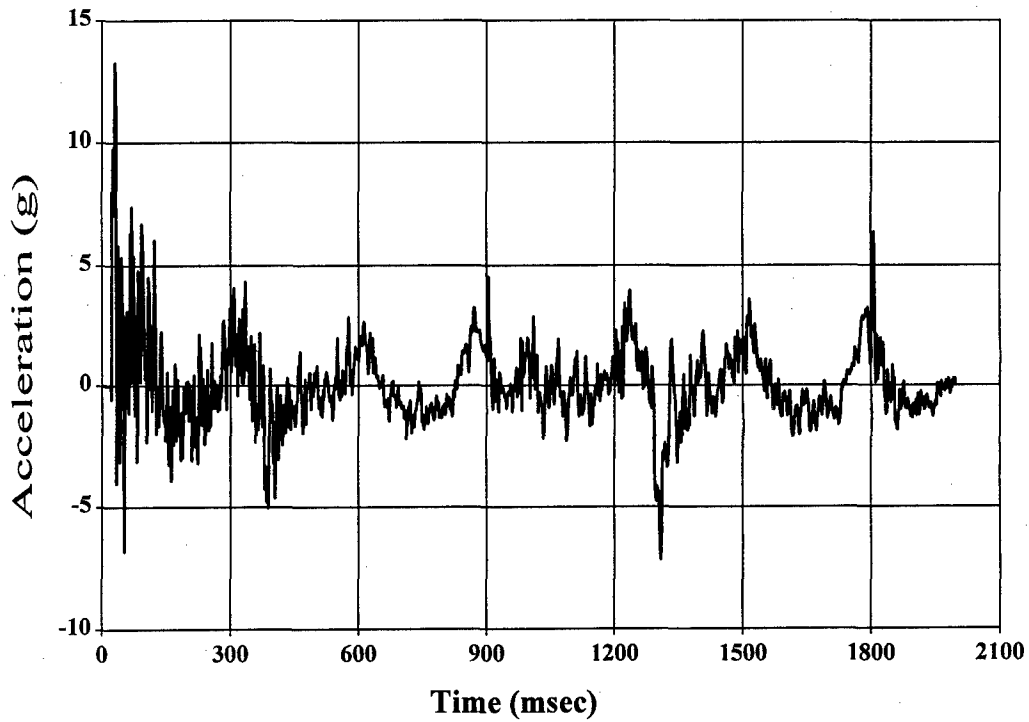
Deck Athwartships Acceleration



NSWC/CD-UERD

03/17/98

Deck Vertical Acceleration



NSWC/CD-UERD

03/17/98

Figure 16. Sample Shock Base Excitation vs. Time

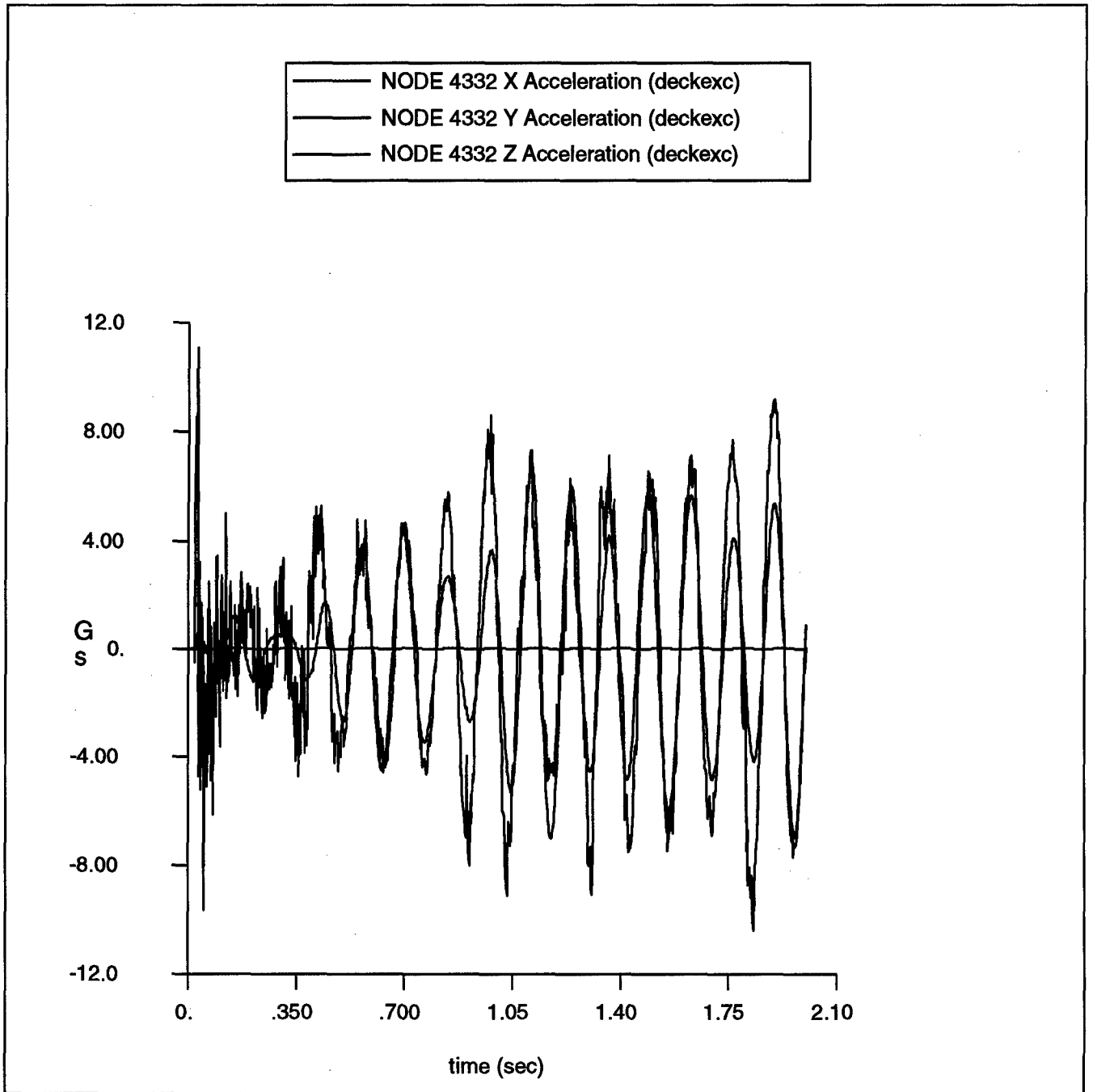


Figure 17. Acceleration Response of Node 4332 (Power Supply).

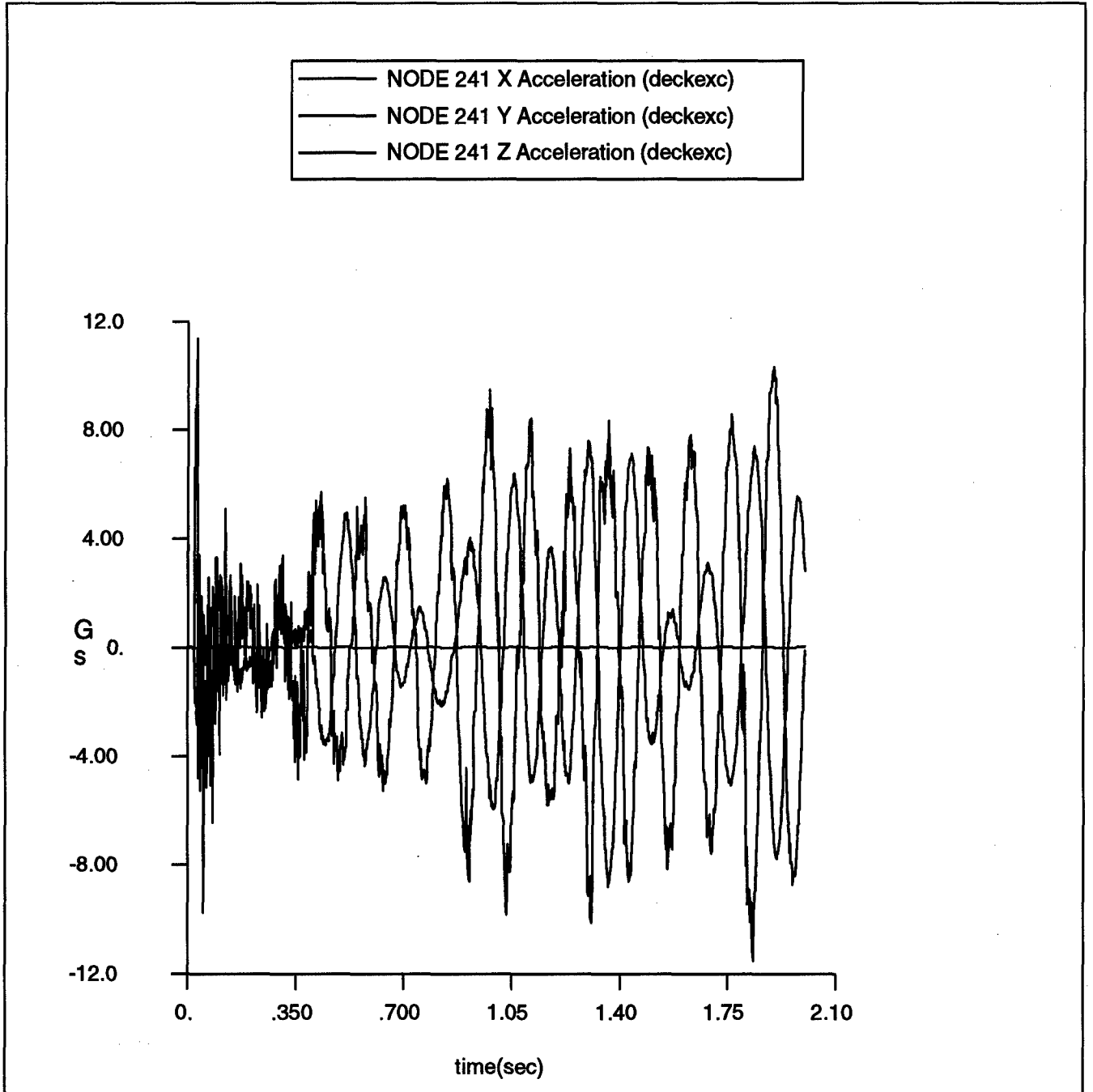


Figure 18. Acceleration Response of Node 241 (Power Distribution Unit)

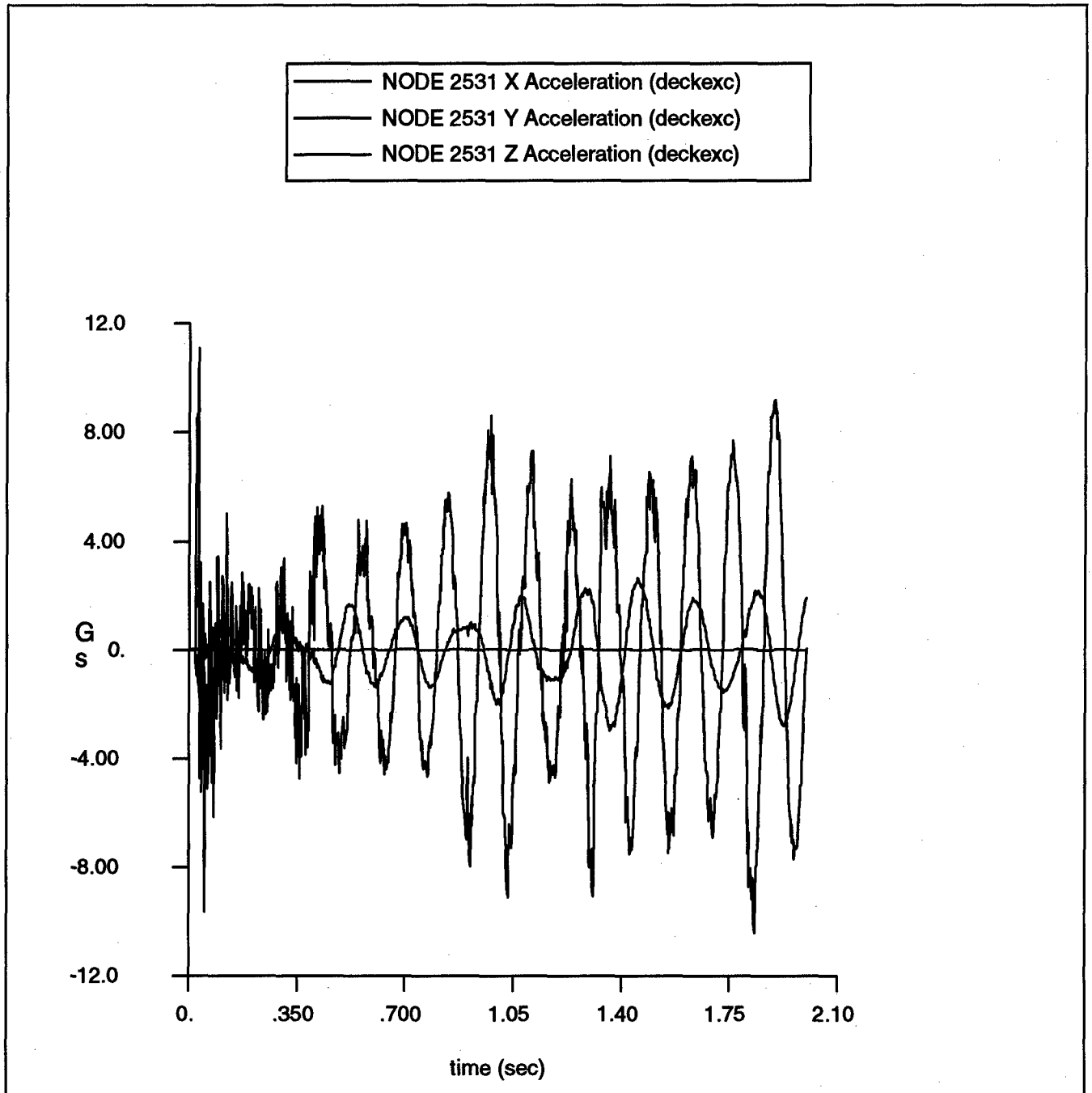


Figure 19. Acceleration Response of Node 2531 (Monitor).

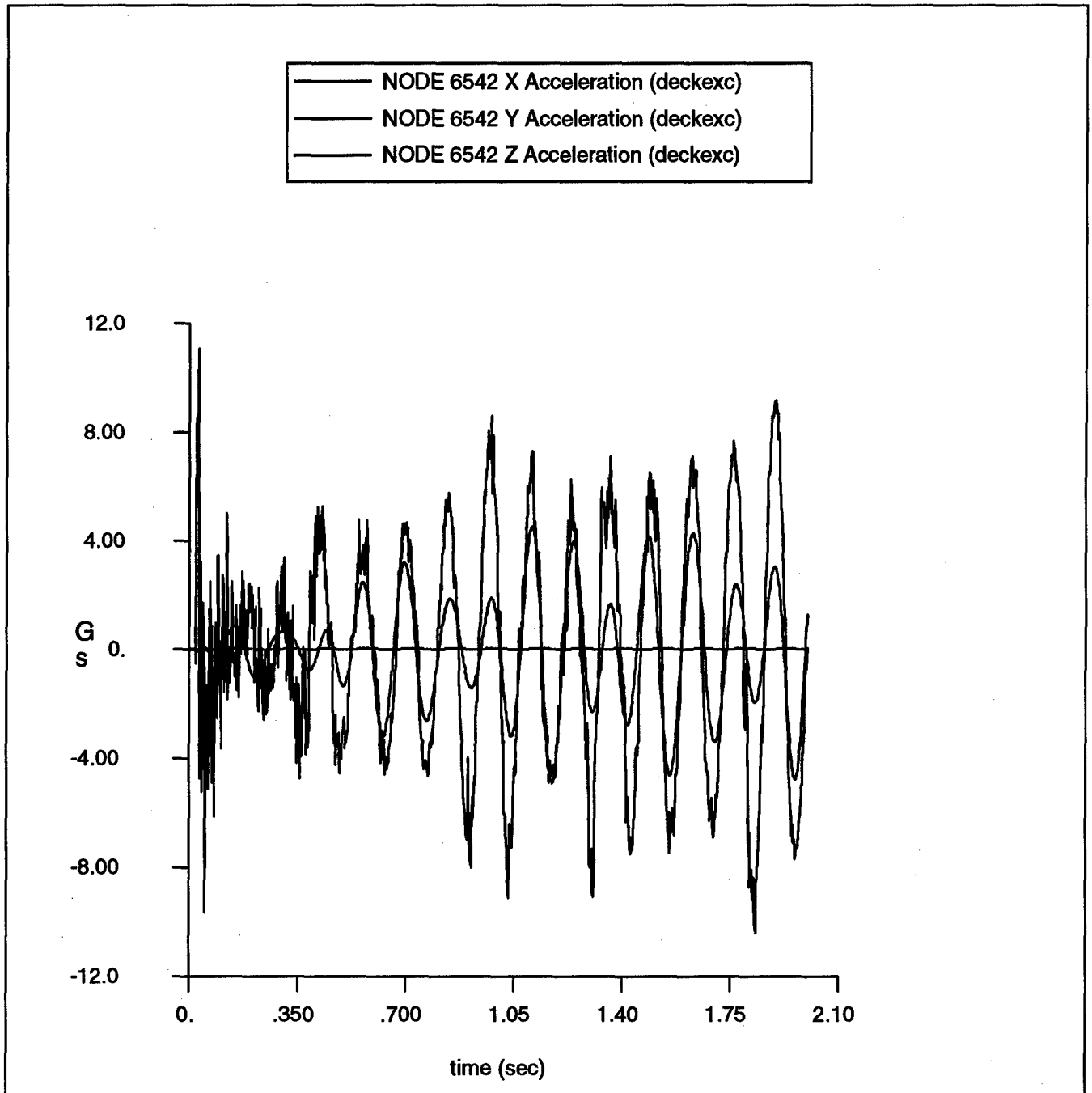


Figure 20. Acceleration Response of Node 6542 (CPU)

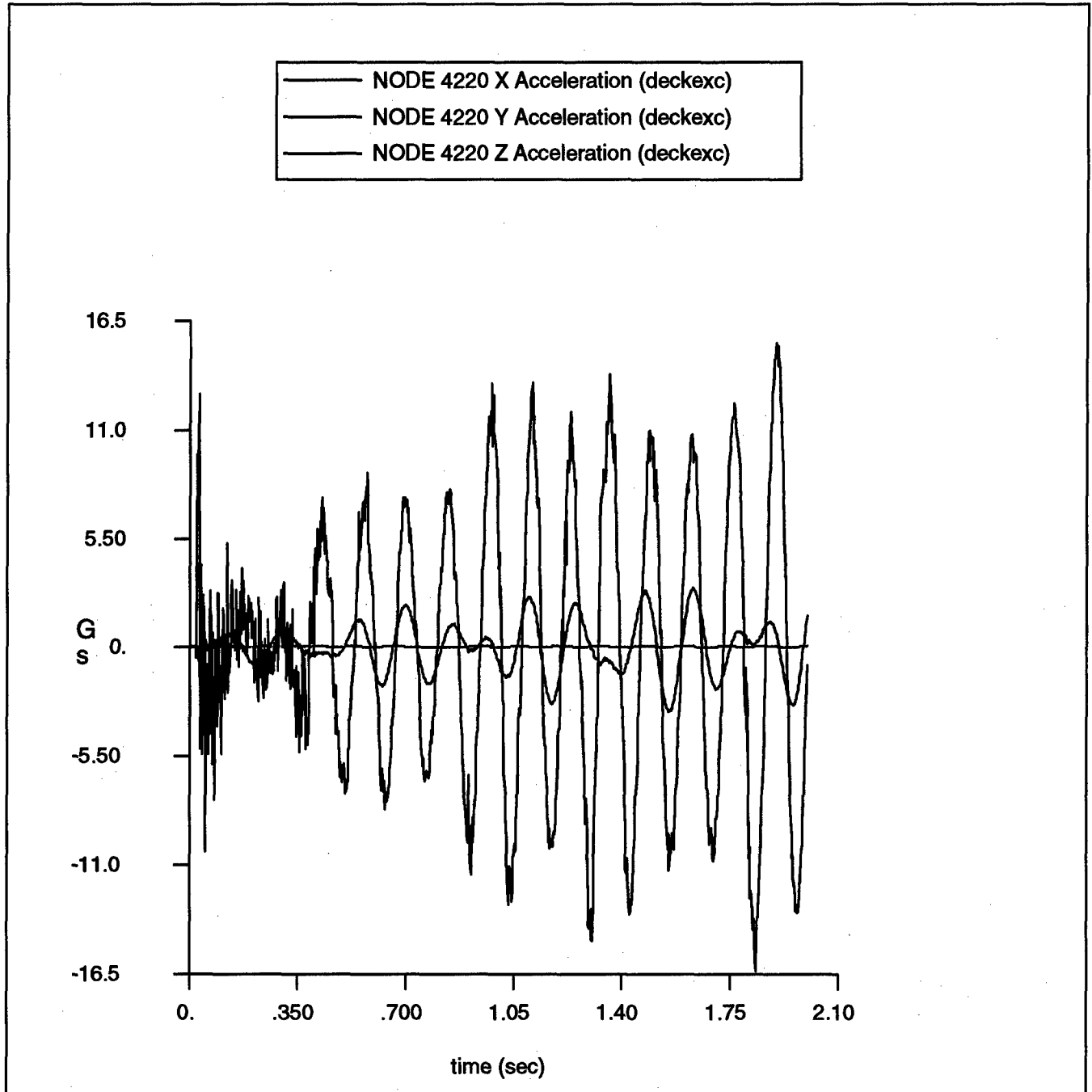


Figure 21. Acceleration Response of Node 4220 (Bullnose)

for the tuned input case, the bullnose values are higher than the internally mounted components due to the lever arm behavior of the bullnose.

Next, Figures 22 and 23 show the acceleration response of two representative nodes on the surface of the cabinet itself. Node 537 is on the bottom of the cabinet and Node 6193 is on the top. As is the case with the electronic components, the response amplitudes increase throughout the time history due to the previously discussed reasons. Note that, however, the maximum values here are generally less than those seen in the electronic components themselves. This situation is interesting in that you generally want the rack itself to experience the larger G forces than the electronic components themselves.

Figures 24 and 25 show the displacement time histories for the shock mounts. As with the case for the halfsine input, there is a significantly larger motion in the Z direction than in the X or Y directions. This is due to two factors. First there is a shock input in the Z direction, the other is the previously mentioned systemic energy transference from the Y to the Z direction. This is also impacted by the Z direction spring stiffness being much less than the Y direction spring stiffness. As stated before, this situation bears close watching with the refinement of the spring mount model to its true non-linear characteristics to ensure that an undesirable response does not result.

The peak acceleration values for all of these discussed nodes for these were less than the combined magnitude of both input shock time histories (about 17.7 G's). However, to ensure that these are the true peak values, longer input time histories are required. The input shock would continue to die down, allowing the racks damping characteristics to mitigate the acceleration response. Responses for longer time periods with an assumed zero input after 2 seconds time were not calculated because these values would not represent the true situation. Also, a longer shock input time record was not available for analysis.

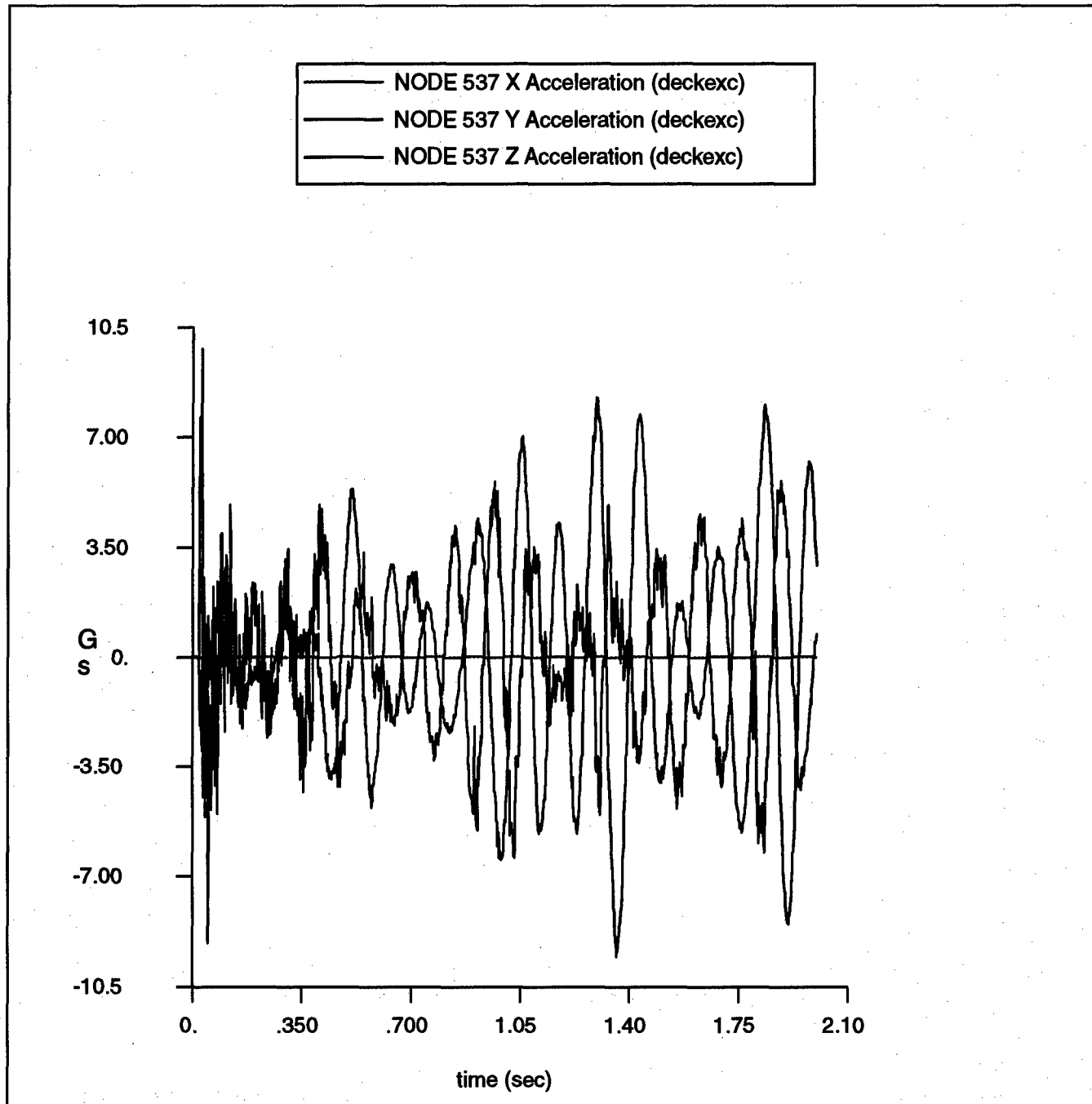


Figure 22. Acceleration Response of Node 537 (Bottom of Cabinet).

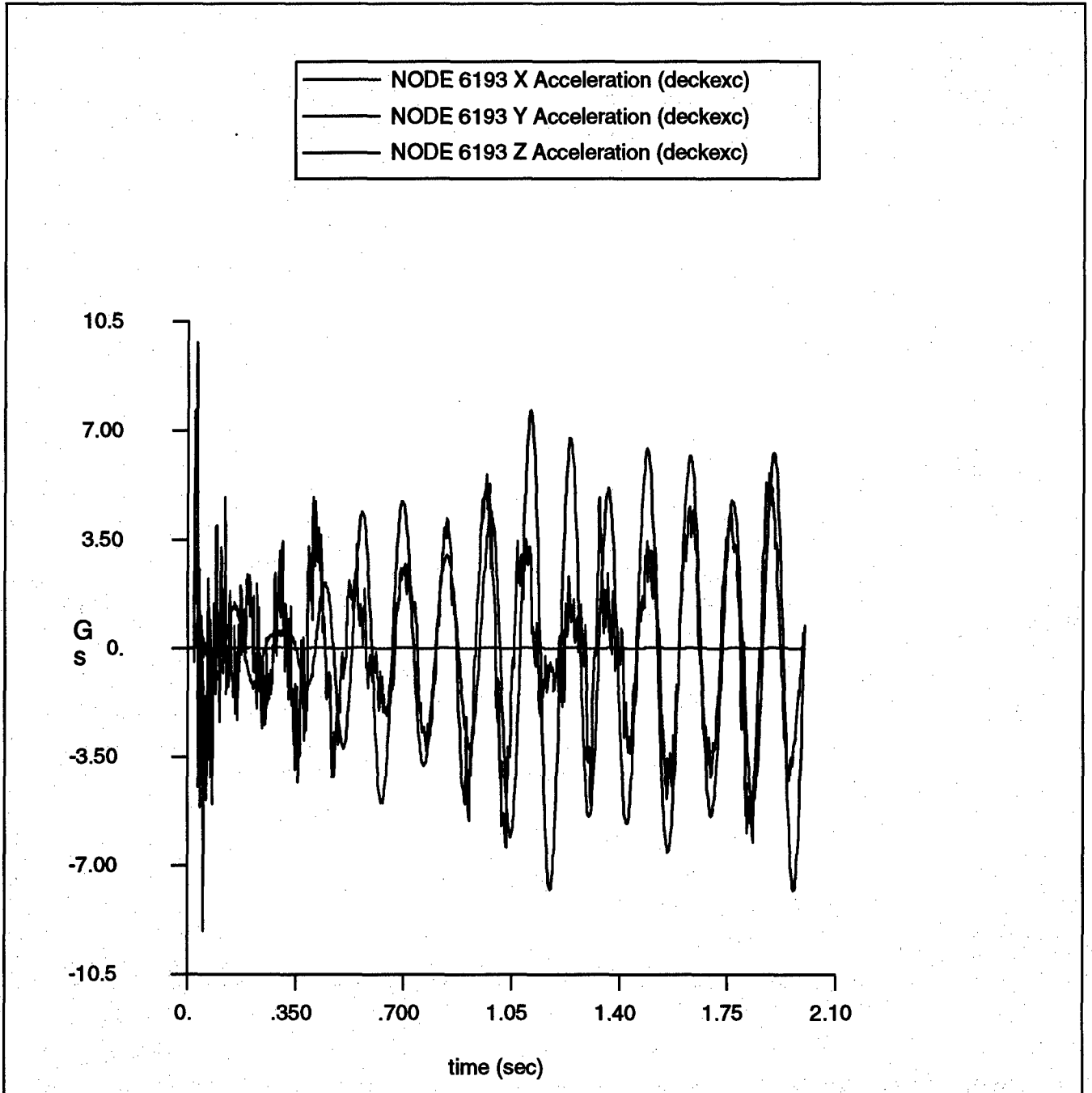


Figure 23. Acceleration Response of Node 6193 (Top of Cabinet)

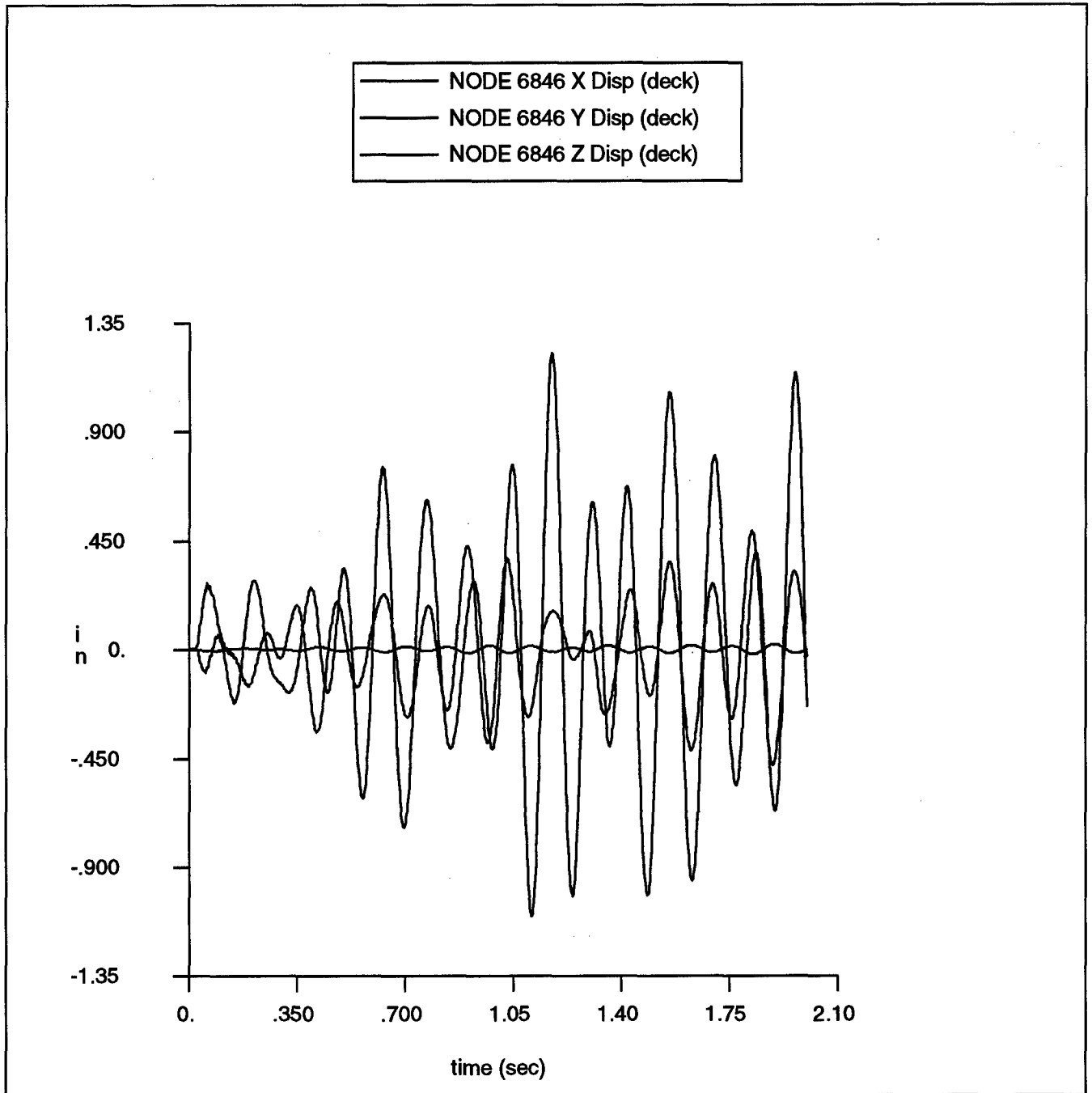


Figure 24. Displacement Response of Node 6846 (Front/Bottom Mount).

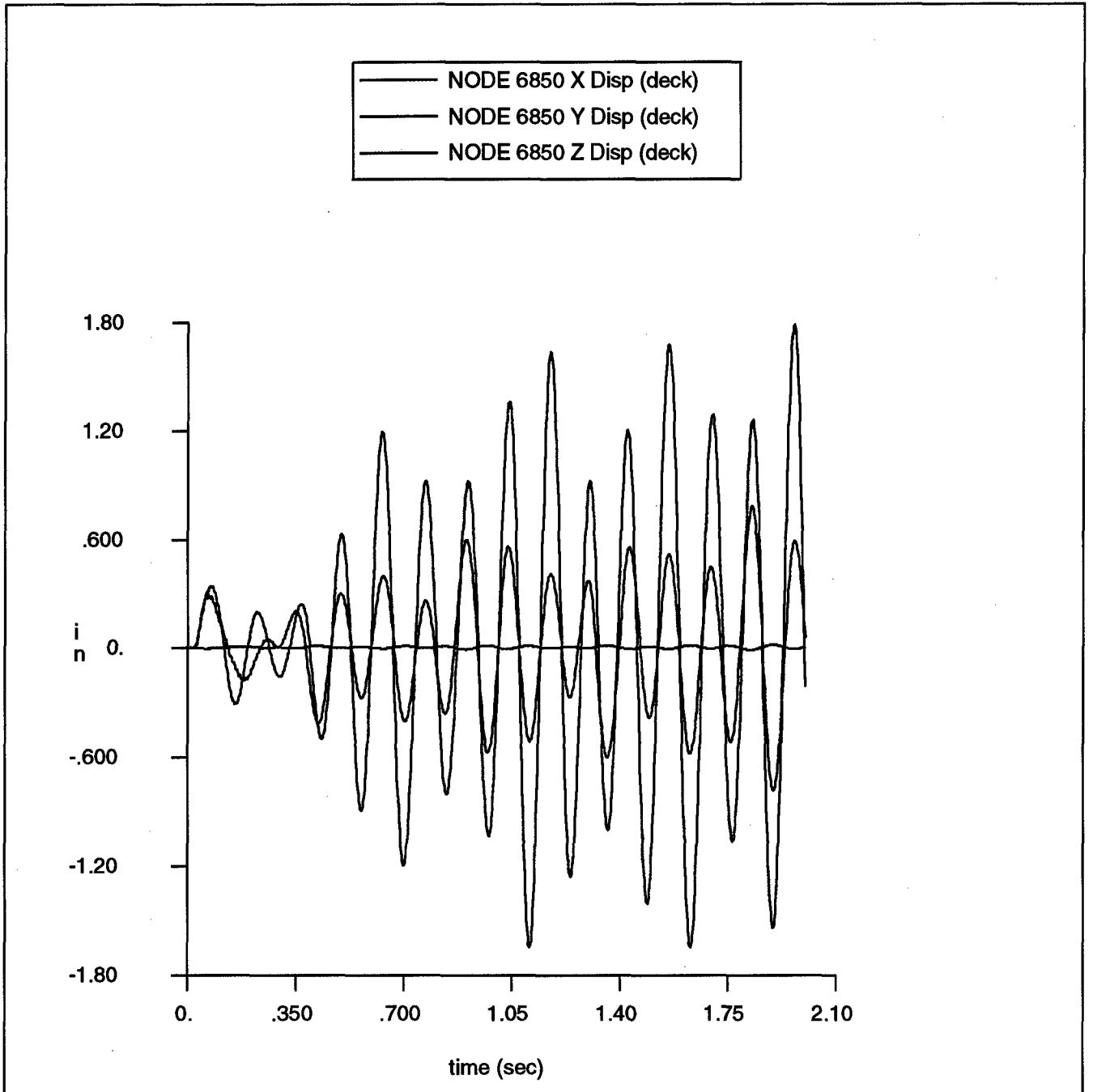


Figure 25. Displacement Response of Node 6850 (Rear/Bottom Mount).

7. DISCUSSIONS

The first simulated shock input was used to represent a large peak short duration shock impulse where the shock input energy is introduced over a very short time period. This is a very abrupt, violent shock which attempts to force a very high peak response in the system by not allowing the isolators enough time to dissipate the energy, thereby transmitting most of the energy to the rack. Once this input peak passes through the system, the response time histories show how rapidly the energy can be dissipated by the mounts and the rack itself.

The second simulated shock input was used to represent more closely an actual shipboard underwater explosion shock. In this case there is a short duration peak at the beginning of the shock input, however shock energy is continually added over a much longer time period. This shock input shows how that although the input peak values subsequent to the initial peak are much less, they can exacerbate the response.

The values obtained from both of these analyses can not be directly compared to each other, but separately they are useful in fully understanding the shock mitigation characteristics of the rack system. Because there is no physical testing result data to compare these values to, the numerical results are still questionable. Care was taken during the modeling process to ensure that all approximations erred to the conservative side. Therefore these values should overestimate the actual physical rack response.

An interesting feature of all the response graphs is that the X direction responses (side-to-side) for both shock inputs were essentially nil compared to the other directions. There are two reasons for this. First, both simulated shock inputs do not apply shock in this direction. The second is that the rack system does not seem to transfer significant input motion from the other directions into this direction. This is likely due to the way in which the rack mounts are situated on the back of the rack. If shock energy is input in the side-to-side direction, however, there will be a significant response in this direction.

One last important modification to the model is required. This is the introduction of the non-linear mount characteristics vice the current linear approximation. Once this is complete, both shock inputs will be simulated on the modified model and a comparison

of the responses to these results as well as a close examination of the deflection of the mounts will be performed. Also a design sensitivity analysis of the rack will be performed to see how certain design characteristics impact the rack's transient response.

Unfortunately, the data obtained for this rack from the MIL901D Medium Weight Shock Machine Test Series could not be used in this model simulation. This is due to the fact that the actual base input seen by the shock mounts themselves was not measured during the testing (shock as transmitted through the anvil and test fixture to the rack).

Finally, the MIL901D Barge Shock Tests for this rack are currently scheduled during April of 1998. Once these are complete, the actual shock input time histories will be used for simulation with the model of the rack. These theoretical results will then be compared to the physical results obtained during the test to prove the viability of the model and the computer based shock simulation technique. Also, these results can be used to improve the rack with respect to shock isolation.

APPENDIX A. GENERAL MODEL CHARACTERISTICS

Height: 72 inches

Width: 24 inches

Depth: 36 inches (exclusive of bullnose)

Weight:

Overall 703.25 lbf

CPU 105 lbf

Monitor 75 lbf

PDU 15 lbf

PS 180 lbf

Bullnose 20 lbf

Center of Gravity: (12.0, 24.8, 18.9) inches

using left, rear, bottom corner of cabinet as origin

Mount spring characteristics:

Front/Bottom X 460 lbf/in

Y 2500 lbf/in

Z 460 lbf/in

Rear/Bottom X 440 lbf/in

Y 2000 lbf/in

Z 440 lbf/in

Back/Upper X 440 lbf/in

Y 440 lbf/in

Z 2000 lbf/in

Structural Damping: 2%

Modal Damping: 2%

LIST OF REFERENCES

1. Guide to Operations and Technical Information Manual for Standard Configuration TAC-4 Rugged Racks, SAIC-Computer Systems, San Diego, Ca.
2. Oesterreich, Mark H. and Shin, Y.S., Modal Analysis of the 72 Inch TAC-4 Ruggedized Rack (CLIN 0003AA), Technical Report NPS-ME-97-005, Naval Postgraduate School, Monterey, Ca., September 1997.
3. FAX from Jansson, Eric, Aeroflex International. Force Deflection Data Curves for CB1400 Series and CB61400 Series Wire Rope Isolators, October 1997.
4. Blakely, Ken, MSC/NASTRAN Basic Dynamic Analysis (V68), MacNeal-Schwendler Corp., Los Angeles, Ca., 1993.
5. Base Accelerometer Data, UERD SITE Phase 3, SHOT 9991, June 1996.

INITIAL DISTRIBUTION LIST

1. Defense Technical Information Center 2
Cameron Station
Alexandria, Virginia 22304-6145
2. Library, Code 52 2
Naval Postgraduate School
Monterey, California 93943-5002
3. Professor Y.S. Shin, Code ME/Sg 2
Department of Mechanical Engineering
Naval Postgraduate School
Monterey, California 93943
4. Lieutenant Mark H. Oesterreich, Code ME/Sg 1
Department of Mechanical Engineering
Naval Postgraduate School
Monterey, California 93943
5. Larry Core, Code D4103 1
NCCOSC, RDT&E Division
TAC Project Office
49184 Transmitter Road
San Diego, CA 92152-7346
6. Russ Eyres, Code D4103 1
NCCOSC, RDT&E Division
TAC Project Office
49184 Transmitter Road
San Diego, CA 92152-7346
7. John Walker, Code D6625 1
Commanding Officer, NCCOSC, RDT&E Div
53560 Hull St
San Diego, CA 92152-5001
8. LCDR Joseph M Iacovetta, Code D3201 1
Commanding Officer, NCCOSC, RDT&E Div
53560 Hull St
San Diego, CA 92152-5001

- | | |
|--|---|
| 9. Adam Simonoff, Code B325
NSWC
Dahlgren, VA 2248-5000 | 1 |
| 10. Wynne Davis
c/o CHET
P.O. Box 280114
Naval Station Mayport, FL 32228 | 1 |
| 11. Mike Winette
NSWCCDSSMDUERD
1445 Crossways Blvd
Cheasapeake, VA 23320 | 1 |
| 12. Research Office, Code 09
Naval Postgraduate School
Monterey, CA 93943 | 1 |